FEW-BODY APPROACHES TO ONE-DIMENSIONAL MANY-BODY SYSTEMS

by

Lawrence Phillips

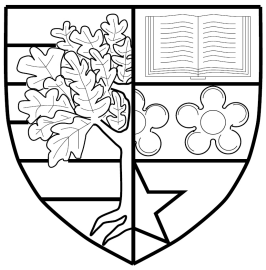

Submitted for the degree of
Doctor of Philosophy

Institute of Photonics and Quantum Sciences
School of Enineering and Physical Sciences
Heriot-Watt University

January 2017

Abstract

This thesis presents results regarding one dimensional many-body quantum systems, obtained by considering the few-body physics of their constituent particles, and through use of traditional quantum mechanical techniques such as scattering theory and the variational principle. Choosing a perspective from which the connection between the microscopic behaviour of the systems' constituents and its macroscopic properties is apparent, we investigate two one-dimensional many-body systems: a flat-banded optical lattice and a fermionic Luttinger liquid. Our choice of approach allows us to give a transparent description of the low-energy physics of both systems. For the former, we find that the low-energy eigenstates may be written down directly in terms of position space creation operators, and that they admit a simple and intuitive interpretation in terms of the position space behaviour of the atoms occupying the lattice. For the latter, we employ few-body scattering theory to investigate a long-held but (until now) untested belief about the parameters appearing in Luttinger's model, a general effective low-energy description of one-dimensional quantum systems. We find this interpretation to be untenable, and give arguments as to how the parameters should correctly be regarded.

Acknowledgements

Thanks firstly to Dr. Manuel Valiente and Prof. Patrik Öhberg for their excellent guidance and supervision, for their unfailing patience and kindness, and for carefully proofreading and correcting this thesis.

Thanks to the rest of the research group for many enlightening (and amusing!) meetings and for generally being good company, and to my other colleagues for providing a welcoming and pleasant working atmosphere.

I acknowledge financial support received from the CM-CDT, and thank everyone involved in its upkeep for their hard work.

Thank you to my family for their ever-reliable love and support, which has been, and remains, a source of great comfort.

List of Publications

This thesis is based on the following publications:

- L. G. Phillips, G. De Chiara, P. Öhberg, and M. Valiente, *Low-energy behaviour of strongly interacting bosons on a flat-band lattice above the critical filling factor*, Phys. Rev. B **91**, 054103.

  Abstract: Bosons interacting repulsively on a lattice with a flat lowest band energy dispersion may, at sufficiently small filling factors, enter into a Wigner-crystal-like phase. This phase is a consequence of the dispersionless nature of the system, which in turn implies the occurrence of single-particle localized eigenstates. We investigate one of these systemsthe sawtooth latticefilled with strongly repulsive bosons at filling factors infinitesimally above the critical point where the crystal phase is no longer the ground state. We find, in the hard-core limit, that the crystal retains its structure in all but one of its cells, where it is broken. The broken cell corresponds to an exotic kind of repulsively bound state, which becomes delocalized. We investigate the excitation spectrum of the system analytically and find that the bound state behaves as a single particle hopping on an effective lattice with reduced periodicity, and is therefore gapless. Thus, the addition of a single particle to a flat-band system at critical filling is found to be enough to make kinetic behavior manifest.

- M. Valiente, L. G. Phillips, N. T. Zinner, P. Öhberg, *Fermionic Luttinger liquids from a microscopic perspective*, arXiv:1505.03519.

  Abstract: We consider interacting one-dimensional, spinless Fermi gases, whose low-energy properties are described by Luttinger liquid theory. We perform a systematic, in-depth analysis of the relation between the macroscopic, phenomenological parameters of Luttinger liquid effective field theory, and the microscopic interactions of the Fermi gas. In particular, we begin by explain-

ing how to model effective interactions in one dimension, which we then apply to the main forward scattering channel – the interbranch collisions – common to these systems. We renormalise the corresponding interbranch phenomenological constants in favour of scattering phase shifts. Interestingly, our renormalisation procedure shows (i) how Luttinger's model arises in a completely natural way – and not as a convenient approximation – from Tomonaga's model, and (ii) the reasons behind the interbranch coupling constant remaining unrenormalised in Luttinger's model. We then consider the so-called intrabranch processes, whose phenomenological coupling constant is known to be fixed by charge conservation, but whose microscopic origin is not well understood. We show that, contrary to general belief and common sense, the intrabranch interactions appearing in Luttinger liquid theory do not correspond to an intrabranch scattering channel, nor an energy shift due to intrabranch interactions, in the microscopic theory. Instead, they are due to interbranch processes. We finally apply our results to a particular example of an exactly solvable model, namely the fermionic dual to the Lieb-Liniger model in the Tonks-Girardeau and super-Tonks-Girardeau regimes.

Contents

Chapter 1

Introduction

Since the early days of quantum condensed matter physics, one-dimensional systems have received a steady stream of interest and study. Their early appeal was down to their simplicity compared with higher-dimensional models: for instance, the key ingredients for a solution of the one-dimensional interacting electron problem were found as early as 1950 [1], whereas physicists required an extra six years - and a completely different theory - to properly understand the same problem in higher dimensions [2]. As another appealing feature, one-dimensional (1D) physics hosts a rich diversity of exactly-solvable models [3], in contrast to higher dimensions, which admit very few such models. This theoretical interest spurred experimentalists on towards realising 1D systems, which they have done in a (by now rather wide) variety of contexts including 1D optical lattices for ultracold atoms [4, 5, 6], quantum wires [7, 8], and carbon nanotubes [9]. Hence, 1D quantum models are of great relevance to modern experimental physics.

One-dimensional systems are also an ideal context within which to explore the relationship between microscopic, few-body physics and macroscopic, condensed matter behaviour. Modern condensed matter theory has become highly sophisticated: elabourate field theories are often employed [10, 11, 12]; algebraic topology is used to study band structure [13, 14]; poorly-understood models are routinely mapped onto other models whose behaviour is well established [15, 16]. This is of course a wonderful development, allowing us to describe an extremely broad class of physical systems and phenomena, and to create and explore novel states of matter. The

role of the underlying microscopic physics is often obscured by treatments of this sort, however. This is not necessarily a problem: often the "fundamental" degrees of freedom - the electrons, atoms, or molecules that make up the system - are not really important degrees of freedom at all, and a clearer picture is obtained by giving up on a description in terms of these constituents and working instead with different, more abstract entities. There are situations, however, where a good understanding of the system is possible in terms its fundamental constituents, and a treatment relying upon more traditional methods and a consideration of the few-body physics occurring in the medium can yield an intuitive, easily-understood, and complete description. In chapter four we present an example of such a system. By using a traditional variational method and by considering a two-body bound state, we are able to very accurately solve for the low-energy behaviour of bosons on a one dimensional lattice, in a regime that has proved inaccessible to sophisticated techniques.

Lack of proper attention to microscopic physics can also lead to misconceptions. In particular, many works on Luttinger's model, a powerful phenomenological model of one dimensional systems, espouse an interpretation of the model's parameters that seems sensible, but has remained untested. To be specific, the phenomenological parameters g_2 and g_4 appearing in Luttinger's model are commonly believed to be related to inter- and intrabranch scattering respectively. By considering the few-body scattering occurring within a dilute Luttinger liquid, we are able to test this interpretation for the first time. We find that g_2 is indeed related to interbranch scattering, whereas, under certain circumstances, the commonly accepted interpretation of g_4 can be shown to be incorrect, casting doubt upon its validity in general. We give a simple argument as to what the correct interpretation should be. Thus, we see that there is still much to be gained from applying well established quantum mechanical methods to, and by considering few-body behaviour within, many-body quantum systems.

Chapter 2

Scattering theory

The systems studied in this thesis have another property in common, alongside one-dimensionality: the macroscopic properties of both systems can be deduced by simplifying the underlying microscopic models, with the simplification taking a similar form in both cases. One ignores the possibility of bound state formation, yielding a model wherein the only interaction processes are scattering processes. This being the case, the realistic two-body interaction may be replaced with any potential yielding the same scattering properties, allowing for a dramatic simplification of the microscopic model. It is necessary to develop a small amount of scattering theory in order to understand this procedure, and we do so in this chapter. After sketching the basic framework, the applications necessary for the rest of this thesis - zero-momentum three-dimensional scattering, which is useful for Bose-Einstein condensates, and one-dimensional scattering, relevant for Luttinger liquids - are treated.

2.1 Basics and motivation

We now introduce some basic scattering theory, following [17]. Given a single-particle Hamiltonian H with a potential V satisfying certain conditions[1], one can decompose the Hilbert space as $\mathcal{H} = \mathcal{H}_B \oplus \mathcal{H}_S$, where B stands for "bound" and S

[1]The conditions are as follows: The potential must fall off faster than r^{-3} at infinity, must be less singular than $r^{-3/2}$ at the origin, and must be continuous, save for a finite number of finite discontinuities.

for "scattering". States in $\mathcal{H}_S$, if evolved by the full Hamiltonian for long enough, behave like free states: their overlap with the potential goes to zero as $t \to \pm\infty$. Let us describe this state of affairs mathematically as

$$e^{-iHt/\hbar}|\psi\rangle \underset{t\to\infty}{\to} e^{-iH_0t/\hbar}|\phi_{\text{out}}\rangle, \tag{2.1}$$

$$e^{-iHt/\hbar}|\psi\rangle \underset{t\to-\infty}{\to} e^{-iH_0t/\hbar}|\phi_{\text{in}}\rangle, \tag{2.2}$$

where $|\psi\rangle \in \mathcal{H}_S$, and the $|\phi\rangle$ can be any states. We therefore have the following picture of a scattering event: the system begins in some state $|\phi_{\text{in}}\rangle$, and evolves freely for some time, until its overlap with the potential becomes significant. The state then evolves under the full Hamiltonian into $|\psi\rangle$, and continues until the effect of the potential is once again negligible, after which it evolves freely as $e^{-iH_0t/\hbar}|\phi_{\text{out}}\rangle$.

Consider now a dilute gas. As we will argue in the next chapter, bound state formation is a rare occurrence in dilute ensembles - provided the initial state does not contain bound states - so that the dynamics of such systems is well-approximated by a series of scattering events, that is, by a series of processes mapping $|\phi_{\text{in}}\rangle \to |\phi_{\text{out}}\rangle$. Let us define a map from in to out asymptotes, $S : |\phi_{\text{in}}\rangle \to |\phi_{\text{out}}\rangle$, and imagine that there are two Hamiltonians H_1 and H_2 which give the same S. Suppose that the gas is prepared in some initial state $|\psi(0)\rangle$, and denote its evolution under H_1 and H_2 by $|\psi_1(t)\rangle$ and $|\psi_2(t)\rangle$ respectively. If the gas is dilute enough so that each two-body scattering process has time to complete, it is clear that $|\psi_1(t)\rangle$ and $|\psi_2(t)\rangle$ will follow one another around the Hilbert space, diverging while scattering events take place, and converging again afterwards (see Fig. 2.1). Thus, if only a few scattering events are taking place at any one time - a few compared with the total number of particles, that is - then the Hilbert space trajectories generated by H_1 and H_2 will agree very closely throughout the evolution. Since a Hilbert space trajectory is the most complete description of a system that one can have, it is clear that H_1 and H_2 will also generate the same macroscopic quantities. It is entirely legitimate, therefore, to replace a complicated Hamiltonian with a less complicated one, provided that the two agree on S (at the appropriate energy) and the system

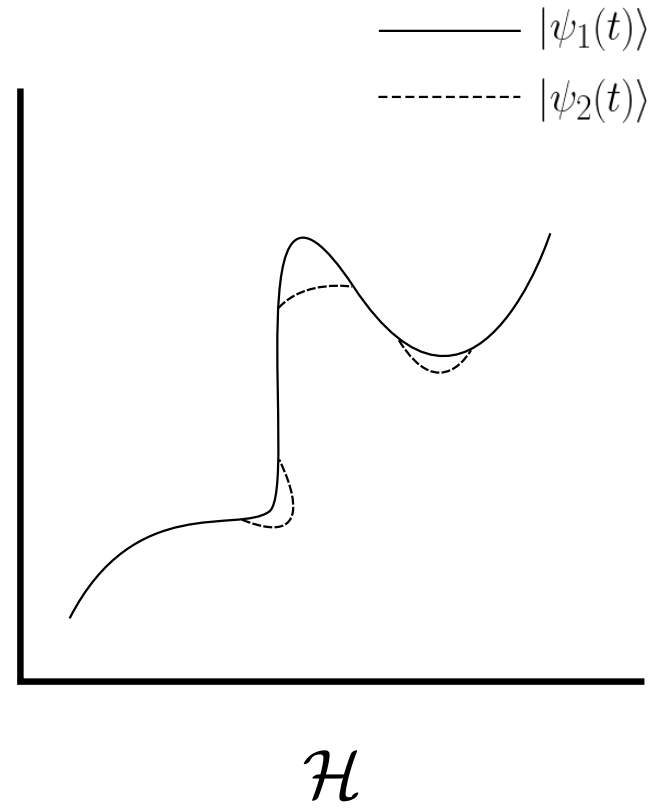

Figure 2.1: Hilbert space trajectories generated by two different Hamiltonians with identical scattering properties. The trajectories differ during times when particles are undergoing scattering; otherwise, they agree.

is dilute. This is a key idea, and it underpins much of the work presented in this thesis[2].

Clearly, it is important to determine whether two given Hamiltonians agree on S. Learning how to do this will be the focus of the next section. As a first step, let us settle some terminology: we will refer to the state $|\psi\rangle$ in Eqs (2.1) and (2.2) as a *scattering* state, and the states $|\phi_{\text{in}}\rangle$, $|\phi_{\text{out}}\rangle$ as *incoming* and *outgoing* states. S is called the S-matrix. Then, let us define maps $\Omega_{\pm}$, called Møller operators, between the scattering state and the incoming and outgoing states: $\Omega_{+}|\phi_{\text{in}}\rangle = \Omega_{-}|\phi_{\text{out}}\rangle =$

[2]As a historical footnote, it is interesting to remark that this idea has been taken to a very extreme limit, known as S-matrix theory [19]. There, the notion of a process, lasting for a finite amount of time, whereby an incoming state becomes an outgoing state, is done away with entirely: one considers only the in and out states to be real, and the mapping between them is the fundamental object of study. The theory was abandoned in the 1970s, but produced string theory as an offshoot.

$|\psi\rangle$. It is intuitively clear that

$$\Omega_+ = \lim_{t\to\infty} e^{-iHt/\hbar} e^{iH_0 t/\hbar}, \tag{2.3}$$

$$\Omega_- = \lim_{t\to\infty} e^{iHt/\hbar} e^{-iH_0 t/\hbar}, \tag{2.4}$$

$$S = \Omega_-^\dagger \Omega_+. \tag{2.5}$$

The above relations between H and S are too complicated to work with directly, due to the matrix exponentiation and the $t \to \infty$ limit. Both of these complications can be removed, however, by exploiting the linearity of the Møller operators and working with the so-called *stationary* scattering states. In order to check whether two S-matrices match, one only needs to know how these states behave outside the influence of the potential, as we will now show.

Consider the action of Ω_+ on some incoming state: $|\phi+\rangle \equiv \Omega_+|\phi_{\text{in}}\rangle$. Writing this in the momentum basis, we have

$$|\phi+\rangle = \Omega_+ \int d^3k\, \phi_{\text{in}}(\mathbf{k})|\mathbf{k}\rangle, \tag{2.6}$$

$$= \int d^3k\, \phi_{\text{in}}(\mathbf{k})|\mathbf{k}+\rangle. \tag{2.7}$$

The $|\mathbf{k}+\rangle$ are called stationary scattering states. They are eigenstates of the full Hamiltonian, with energies $\epsilon(k) = \hbar^2k^2/2m$ (with $k \equiv |\mathbf{k}|$, and assuming the usual dispersion relation). Now, to find the outgoing state that emerges from $|\phi_{\text{in}}\rangle$, one must act with $\Omega_-^\dagger$, mapping $|\phi+\rangle$ to the far future under the full Hamiltonian, and then back to the present under H_0. After the first part of that operation, the overlap between the state and the potential will be vanishingly small. Thus, in order to carry out the second step, one needs only to know the $|\mathbf{k}+\rangle$ outside of the range of the potential. Also, since the $|\mathbf{k}+\rangle$ are eigenstates of H, we have $e^{-iHt/\hbar}|\mathbf{k}+\rangle = e^{-i\epsilon(k)t/\hbar}|\mathbf{k}+\rangle$, regardless of the form of $|\mathbf{k}+\rangle$. These facts together mean that the S-matrix depends only on the $|\mathbf{k}+\rangle$ outside of the range of the potential, or, equivalently, on the asymptotic behaviour $\langle\mathbf{x}|\mathbf{k}+\rangle_{r\to\infty}$ (where $r \equiv |\mathbf{x}|$). So, in order to check whether two models have the same scattering properties, one

need only compare the asymptotic forms of their stationary scattering states. This is vastly simpler than working with Eqs (2.3), (2.4) and (2.5) directly. Let us now develop equations allowing us to perform this comparison. We have

$$\Omega_+|\mathbf{k}\rangle = |\mathbf{k}\rangle + \lim_{t\to\infty}\int_0^{-t/\hbar} d\tau\, \frac{d}{d\tau} e^{iH\tau}e^{iH_0\tau}|\mathbf{k}\rangle \tag{2.8}$$

$$= |\mathbf{k}\rangle + i\int_0^{\infty} d\tau\, e^{-iH\tau}Ve^{iH_0\tau}|\mathbf{k}\rangle, \tag{2.9}$$

$$= |\mathbf{k}\rangle + i\int_0^{\infty} d\tau\, e^{-i(H-\epsilon(k))\tau}V|\mathbf{k}\rangle. \tag{2.10}$$

The integral in Eq. (2.10) does not converge. It is possible to make it convergent without affecting any physics, however: simply introduce a small time dependence in the potential as $V \to e^{-\eta t}V$, with $0 < \eta \ll 1$. Since the effect of the potential vanishes at large times for any scattering event, one can always choose an η small enough so that $e^{-\eta t}$ is negligible whilst V plays a role. Adding the damping term and performing the integration yields

$$\Omega_+|\mathbf{k}\rangle = |\mathbf{k}\rangle + \lim_{\eta\to 0^+}(\epsilon(k) + i\eta - H)^{-1}V|\mathbf{k}\rangle, \tag{2.11}$$

$$\equiv |\mathbf{k}\rangle + \lim_{\eta\to 0^+} G(\epsilon(k) + i\eta)V|\mathbf{k}\rangle, \tag{2.12}$$

where in the last equation we have defined the interacting Green's function $G(z)$. [3] It is easily seen that $G(z)$ satisfies

$$G(z) = G_0(z) + G_0(z)VG(z), \tag{2.13}$$

where G_0 is the non-interacting Green's function, $G_0(z) = (z - H_0)^{-1}$. Also, it is useful to define another operator, the T-matrix, in terms of $G(z)$ as

$$T(z) = V + VG(z)V. \tag{2.14}$$

[3] By the same kind of argument, one sees that $\Omega_-|\mathbf{k}\rangle = |\mathbf{k}\rangle + \lim_{\eta\to 0^-} G(\epsilon(k) + i\eta)|\mathbf{k}\rangle$.

The last two equations together imply that

$$G_0(z)T(z) = G(z)V, \tag{2.15}$$

which can be used in Eq. (2.12) to obtain the so-called Lippmann-Schwinger equation for $|\mathbf{k}+\rangle$,

$$|\mathbf{k}+\rangle = |\mathbf{k}\rangle + G_0(\epsilon(k) + i0^+)V|\mathbf{k}+\rangle, \tag{2.16}$$

which, after taking the position representation and performing a contour integral, reads

$$\psi_{\mathbf{k}}(\mathbf{x}) = \phi_{\mathbf{k}}(\mathbf{x}) - \frac{m}{2\pi\hbar^2}\int d^3x' \, \frac{e^{ik|\mathbf{x}-\mathbf{x}'|}}{|\mathbf{x}-\mathbf{x}'|}V(\mathbf{x}')\psi_{\mathbf{k}}(\mathbf{x}'), \tag{2.17}$$

where $\psi_{\mathbf{k}}(\mathbf{x}) = \langle \mathbf{x}|\mathbf{k}+\rangle$ and $\phi_{\mathbf{k}}(\mathbf{x}) = \langle \mathbf{x}|\mathbf{k}\rangle$. We are now in a position to inspect the asymptotic form of $|\mathbf{k}+\rangle$: it is

$$\psi_{\mathbf{k}}(\mathbf{x})_{r\to\infty} = \phi_{\mathbf{k}}(\mathbf{x}) - \frac{m}{2\pi\hbar^2}\frac{e^{ikr}}{r}\int d^3x' e^{-ik\hat{\mathbf{x}}\cdot\mathbf{x}'}V(\mathbf{x}')\psi_{\mathbf{k}}(\mathbf{x}'), \tag{2.18}$$

$$\equiv \frac{1}{(2\pi)^{3/2}}\left(e^{i\mathbf{k}\cdot\mathbf{x}} + f(k\hat{\mathbf{x}},\mathbf{k})\frac{e^{ikr}}{r}\right). \tag{2.19}$$

where $\hat{\mathbf{x}} = \mathbf{x}/r$. One sees that the stationary scattering states have a very simple asymptotic form, containing only an incident wave part, $\phi_{\mathbf{k}}$, and an outgoing spherical wave, modulated by a function that depends only on the angle between x and the origin, and on the incoming momentum vector $\mathbf{k}$. Thus, we have reduced the task of checking whether two theories have the same scattering properties to that of calculating the modulating function $f(k\hat{\mathbf{x}},\mathbf{k})$, which is called the *scattering amplitude*. In the next section, we investigate this amplitude for particles at low energies.

2.2 Ultracold Scattering

A prominent application of the ideas outlined above is found in the theory of interacting Bose-Einstein condensates. There, one exploits the simplicity of zero-momentum scattering and replaces the complicated interatomic interaction with a much simpler

one. We will explain this procedure in more detail when we consider optical lattices in the next section; for now, our concern is to show that scattering at very low energies depends only on a single parameter, the *scattering length*.

When attempting to solve a problem, it is often a good idea to begin by reducing the size of the space of possible solutions. In the present case, the problem of scattering at low energies, the quantization of angular momentum provides a natural way of achieving such a reduction. States with nonzero angular momentum must pay a finite energy cost, and thus may be eliminated from low-energy considerations. To see this, consider the Schrödinger equation in spherical coordinates

$$\left(-\frac{\hbar^2}{2\mu r^2}\left[\partial_r(r^2\partial_r) - \hat{\mathbf{L}}^2\right] + V(r)\right)\psi(r,\theta,\phi) = E\psi(r,\theta,\phi) \tag{2.20}$$

where we have separated center of mass and relative coordinates, and are focusing on the relative part. Also, we have assumed that the potential depends only on the interparticle distance r, as is often the case in atomic physics. The fact that the potential is spherically symmetric allows one to obtain a purely radial equation. Since $\hat{\mathbf{L}}$ commutes with H, all eigenstates of H must also be eigenstates of $\hat{\mathbf{L}}$, which fixes the angular dependence of the wavefunction: one has

$$\psi(r,\theta,\phi) = R(r)Y_{lm}(\theta,\phi), \tag{2.21}$$

where the Y_{lm} are spherical harmonics, eigenfunctions of $\hat{\mathbf{L}}$ with eigenvalue $l(l+1)$. Using this form for the wavefunction in Eq. (2.20), the Y_{lm} may be eliminated, and we obtain

$$\left(-\frac{\hbar^2}{2\mu r^2}\left[\partial_r(r^2\partial_r) - l(l+1)\right] + V(r)\right)R(r) = ER(r). \tag{2.22}$$

Thus, a state with nonzero angular momentum experiences a centrifugal barrier $\propto 1/r^2$. This barrier will inevitably increase the energy of the eigenstates; thus, at low energies, we are justified in restricting the Hilbert space to states with $l = 0$. This drastic simplification leads to a very simple form for the scattering amplitude. In order to see why, first note that, in the case of a spherically symmetric potential, the orbital angular momentum operator $\hat{\mathbf{L}}$ commutes with the S-matrix. This is

due to the role of $\hat{\mathbf{L}}$ as the generator of rotations. It is intuitively obvious that the S-matrix commutes with rotations for a spherically symmetric potential: rotating the system before a scattering event or doing so afterwards results in the same outgoing state. Since the S-matrix commutes with rotations, it must commute with their generator. Also, since scattering conserves kinetic energy asymptotically, the S-matrix commutes with H_0. Therefore, S shares simultaneous eigenstates with $\hat{\mathbf{L}}^2$, $\hat{L}_z$, and H_0. Since the latter three operators define a complete set of commuting observables, their eigenstates $\{|E, l, m\rangle\}$ form a basis for $\mathcal{H}$, and S is diagonal in this basis. Thus, S has the following representation:

$$S = \int dE \sum_{l,m} s_l(E)|E, l, m\rangle\langle E, l, m|. \tag{2.23}$$

The eigenvalues of S are independent of m, as can be seen from the fact that S commutes with the ladder operators for l. Also, the unitarity of S [4] implies that $s_l(E)$ must satisfy $|s_l(E)| = 1$, so we may for convenience write it as $s_l(E) = e^{2i\delta_l(E)}$. Now, in the previous section we argued that S depends only on the asymptotic form of the stationary scattering states. This is reflected in the fact that S is completely determined by the scattering amplitude f; the two are related via

$$\langle \mathbf{p}'|(S-1)|\mathbf{p}\rangle = \frac{i}{2\pi m}\delta(\epsilon(p) - \epsilon(p'))f(\mathbf{p}', \mathbf{p}). \tag{2.24}$$

Using this relation together with Eq. (2.23), one obtains

$$f(\mathbf{p}', \mathbf{p}) = \sum_{l=0}^{\infty}(2l+1)f_l(\epsilon(p))P_l(\cos\theta), \tag{2.25}$$

where θ is the angle between $\mathbf{p}$ and $\mathbf{p}'$, P_l is the l-th Legendre polynomial, and we have defined the partial wave amplitude

$$f_l(E) \equiv \frac{s_l(E) - 1}{2ip} = \frac{e^{i\delta_l(E)}\sin\delta_l(E)}{p}. \tag{2.26}$$

The sum over l in Eq. (2.25) comes from the expansion of S in terms of angular

[4] This follows directly from the definition in terms of Møller operators: $S^\dagger = \Omega_+^\dagger\Omega_- = S^{-1}$.

momentum states; thus, at low energies, only the $l = 0$ term need be retained. Dropping all the other terms, then, one finds a very simple form for the scattering amplitude at low energies:

$$f(p) = \frac{e^{i\delta_0(\epsilon(p))} \sin \delta_0(\epsilon(p))}{p}. \tag{2.27}$$

In the ultracold regime, the majority of particles have momentum close to zero. Therefore, scattering in an ultracold gas will be controlled by $\lim_{p\to 0} f(p) \equiv -a$. This limit can be shown to exist [18] and is called the scattering length "a". It completely determines the scattering properties of atoms at very low energies, a fact that we shall make use of in the next chapter.

2.3 Identical particles and principal value operators

When calculating the scattering properties of a system of identical particles with time-reversal-invariant interactions, it is possible to use a simplified formalism, in which one may "ignore" the infinitesimal imaginary parts in the arguments of the on-shell Green's functions and T-matrix. In Chapter 6 we will employ this idea to simplify a rather long calculation as well as several proofs. The formalism is interesting from a practical point of view, since it allows one to ignore the imaginary parts in the Lippmann-Schwinger equation. For ease of notation we particularise to one dimension in this section, but the arguments presented here also hold in three dimensions.

The scattering of a pair of identical particles is completely determined by the equation

$$|\tilde{p}+\rangle = \hat{\Lambda}|p\rangle + G_0(E_p + i0^+)T(E_p + i0^+)\hat{\Lambda}|p\rangle, \tag{2.28}$$

$$\equiv \hat{\Lambda}|p\rangle + G_{0+}(E_p)T_+(E_p)\hat{\Lambda}|p\rangle, \tag{2.29}$$

where $\hat{\Lambda}$ is the (anti)symmetrisation operator for bosons (fermions), and $|p\rangle$ is an

eigenstate of the relative momentum operator for a pair of particles. We also define $T_-(E_p) \equiv T(E_p + i0^-)$, and make the analogous definition for G_{0-}. Note that if we wish $\hat{\Lambda}$ to preserve norm, it must be a non-linear operator, defined as

$$\hat{\Lambda}|\psi\rangle \equiv \frac{(1 \pm \mathbb{P})|\psi\rangle}{\sqrt{\langle\psi|(1 \pm \mathbb{P})^2|\psi\rangle}} \tag{2.30}$$

$\mathbb{P}$ is the parity operator. Now, any operator $\mathcal{O}$ that is invariant under parity satisfies $\mathcal{O}\hat{\Lambda} = \hat{\Lambda}\mathcal{O}\hat{\Lambda}$:

$$\langle p'|\mathcal{O}\hat{\Lambda}|p\rangle = \frac{1}{2}\langle p|(\mathcal{O} + \mathbb{P}^\dagger\mathcal{O}\mathbb{P})\hat{\Lambda}|p\rangle \tag{2.31}$$

$$= \frac{1}{2}(\langle p'|\mathcal{O}\hat{\Lambda}|p\rangle + \langle -p'|\mathcal{O}\hat{\Lambda}|-p\rangle) \tag{2.32}$$

$$= \frac{1}{2}(\langle p'| \pm \langle -p'|)\mathcal{O}\hat{\Lambda}|p\rangle \tag{2.33}$$

$$= \langle p'|\hat{\Lambda}\mathcal{O}\hat{\Lambda}|p\rangle, \tag{2.34}$$

where in the last line we have used the fact that $\sqrt{\langle p|(1 \pm \mathbb{P})^2|p\rangle} = 2$. If the potential is symmetric, both the T-matrix and the Green's function will be parity invariant, and thus

$$|\tilde{p}+\rangle = \hat{\Lambda}|p\rangle + \hat{\Lambda}G_{0+}(E_p)\hat{\Lambda}T_+(E_p)\hat{\Lambda}|p\rangle \tag{2.35}$$

$$\equiv \hat{\Lambda}|p\rangle + \mathcal{G}_0(E_p)\mathcal{T}(E_p)|p\rangle, \tag{2.36}$$

where $\mathcal{G}_0(E) = \hat{\Lambda}G_{0+}(E)$ and $\mathcal{T}(E) = \hat{\Lambda}T_+(E)\hat{\Lambda}$. The motivation for defining $\mathcal{G}_0$ and $\mathcal{T}$ - which we will refer to as *principal value* operators, for reasons that will soon become clear - is that they turn out to be simpler than their non-principal-value counterparts. To see this, it is useful to introduce the time reversal operator $\mathbb{T}$, defined via

$$\mathbb{T}|p\rangle = |-p\rangle, \tag{2.37}$$

$$\mathbb{T}|x\rangle = |x\rangle. \tag{2.38}$$

By considering inner products between position and momentum states, one may

establish that $\mathbb{T}$ is *anti-unitary*, that is, norm preserving and anti-linear. Anti-linearity implies that $\langle\phi_A|\mathbb{T}\phi_B\rangle = \langle\phi_A\mathbb{T}^\dagger|\phi_B\rangle^*$, which gives the rather strange relation, $\mathbb{T}i|\psi\rangle = -i\mathbb{T}|\psi\rangle$. Therefore, assuiming a time-reversal-invariant Hamiltonian, we have $\mathbb{T}G_{0\pm} = G_{0\mp}\mathbb{T}$, and similarly $\mathbb{T}T_\pm = T_\mp\mathbb{T}$. Thus,

$$\langle p'|\hat{\Lambda}G_{0+}(E_p)\hat{\Lambda}|p\rangle = \frac{1}{2}\langle p'|\hat{\Lambda}(G_{0+}(E_p) + \mathbb{T}^\dagger G_{0+}(E_p)\mathbb{T})\hat{\Lambda}|p\rangle, \tag{2.39}$$

$$= \frac{1}{2}\langle p'|(G_{0+}(E_p) + G_{0-}(E_p))\hat{\Lambda}|p\rangle, \tag{2.40}$$

where we have used the fact that $\hat{\Lambda}|p\rangle = -\mathbb{T}\hat{\Lambda}|p\rangle$. Comparing the above with Eq. (2.36), we obtain

$$\mathcal{G}_0(E) = \frac{1}{2}[G_{0+}(E) + G_{0-}(E)]. \tag{2.41}$$

To see the simplification offered by working with $\mathcal{G}_0$, consider the matrix element

$$\langle p'|G_{0\pm}(E)|p\rangle = \langle p'|\frac{1}{E - H_0 + i0^\pm}|p\rangle. \tag{2.42}$$

Noting that G_0 only makes sense as an integral kernel, and using the Sokhotski-Plemelj theorem [20], we can write

$$\langle p'|G_{0\pm}(E)|p\rangle = 2\pi\delta(p'-p)\left[\mathcal{P}\left(\frac{1}{E-\epsilon(p)}\right) \mp i\pi\delta(E-\epsilon(p))\right], \tag{2.43}$$

$$\Rightarrow \langle p'|\mathcal{G}_0(E)|p\rangle = 2\pi\delta(p'-p)\mathcal{P}\left(\frac{1}{E-\epsilon(p)}\right), \tag{2.44}$$

where $\mathcal{P}$ denotes principal value integration - hence the name principal value operators. We see that the imaginary part, which is a needless complication containing no information about the scattering of identical particles, does not appear in $\mathcal{G}_0$. As for the $\mathcal{T}$-matrix, using Eqs (2.14) and (2.15), we have

$$\langle p'|\hat{\Lambda}T_+(E_p)\hat{\Lambda}|p\rangle = \langle p'|\hat{\Lambda}\big[V + VG_{0+}(E_p)T_+(E_p)\big]\hat{\Lambda}|p\rangle \tag{2.45}$$

$$= \langle p'|\big[V_p + V_p\hat{\Lambda}G_{0+}(E_p)\hat{\Lambda}T_+(E_p)\hat{\Lambda}\big]|p\rangle. \tag{2.46}$$

where we have defined $V_p = \hat{\Lambda}V$. Thus, the on-shell $\mathcal{T}$-matrix obeys a Lippmann-

Schwinger equation

$$\langle p'|\mathcal{T}(E_p)|p\rangle = \langle p'|\big[V_p + V_p\mathcal{G}_0(E_p)\mathcal{T}(E_p)\big]|p\rangle. \tag{2.47}$$

Finally, one may use equations (2.36) and (2.14) to obtain an implicit equation for $|\tilde{p}+\rangle$,

$$|\tilde{p}+\rangle = \hat{\Lambda}|p\rangle + \mathcal{G}_0 V_p|\tilde{p}+\rangle. \tag{2.48}$$

It is convenient to work with the equations (2.36), (2.47), and (2.48) rather than the usual Lippmann-Schwinger equations when treating the scattering of identical particles, and we will make use of this formalism in the next section, and in chapter 6.

2.4 Scattering in one dimension

The idea outlined in section 2.1 is ideally suited to the study of one-dimensional quantum systems. This is because one-dimensional scattering for identical particles always occurs in a single "angular momentum" channel - even or odd wave - and is thus controlled by a single parameter, no matter what the energy, in contrast to higher dimensions where this is true only at low energies. Later on, we will describe an application to a one dimensional system, and therefore it will be helpful to establish some relations in one dimensional scattering at this point. We work with identical fermions, since this will be our application domain; the bosonic case is analogous.

To begin with, we calculate the position-space representation of the one-dimensional principal value Green's function $\mathcal{G}_0(E)$:

$$\langle x|\mathcal{G}_0(E_p)|x'\rangle = \int dp'\, \langle x|\mathcal{G}_0(E_p)|p'\rangle\langle p'|x'\rangle \tag{2.49}$$

$$= \lim_{\eta\to 0^+} \frac{m}{\hbar^2\pi} \int dp'\, e^{ip'(x-x')} \left(\frac{1}{p^2 + i\eta - p'^2} + \frac{1}{p^2 - i\eta - p'^2}\right). \tag{2.50}$$

This is easily evaluated by contour integration: one closes the contour in either the upper or the lower half plane, depending on the sign of $x - x'$, and each term picks

up one of its two poles, depending on the sign of $i\eta$. We obtain

$$\langle x|\mathcal{G}_0(E_p)|x'\rangle = \frac{m}{\hbar^2|p|}\sin(|p(x-x')|). \tag{2.51}$$

This leads to the following form for the stationary scattering states:

$$\psi_p(x) = \frac{i\sin(px)}{\sqrt{2\pi}} + \frac{im}{\hbar^2|p|}\int dx' \sin(|p(x-x')|)V_p(x')\mathrm{Im}[\psi_p(x')], \tag{2.52}$$

where we have used the fact that $\psi_p(x)$ is purely imaginary for identical fermions (as can be seen by iterating 2.48) to pull out its phase in the second term, for later convenience. Let us inspect the $r \to \infty$ limit of $\psi_p(x)$ (where $r = |x|$),

$$\psi_p(x)_{r\to\infty} = \frac{i\sin(px)}{\sqrt{2\pi}} - \frac{im}{\hbar^2|p|}\mathrm{sgn}(x)\cos(|p|x)\int dx' \sin(|p|x')V_p(x')\mathrm{Im}[\psi_p(x')] \tag{2.53}$$

$$\equiv \frac{i}{\sqrt{2\pi}}\big(\sin(px) - \mathrm{sgn}(x)\tan(\theta_p)\cos(|p|x)\big) \tag{2.54}$$

$$= \frac{i\,\mathrm{sgn}(x)}{\sqrt{2\pi}}\ \frac{\sin(p|x|+\theta_p)}{\cos(\theta_p)}. \tag{2.55}$$

We see that one-dimensional stationary scattering states have a particularly simple asymptotic form: the "incoming" sine wave has its phase shifted by an amount θ_p, its magnitude scaled by an irrelevant factor $1/\cos(\theta_p)$, and nothing more. Thus, the phase shift θ_p completely determines the scattering physics for any given pair of identical particles in one dimension[5]. In treating a dilute one-dimensional system, then, one may replace the realistic interaction with an effective potential that reproduces the exact phase shift (at a given energy), and can expect to obtain dynamics close to that of the realistic model at any energy. We will apply this idea to Luttinger liquids in Chapter 6.

[5]In the case of distinguishable particles, two phase shifts are required: one for even, and the other for odd, waves.

Chapter 3

Optical lattices

In the next chapter we will consider the behaviour of a bosonic atomic gas in the presence of an optical lattice, and so here we give a sketch of the basic principles underlying the theory of such systems, and derive their basic model, the Bose-Hubbard model. The optical lattice idea emerged during the early 1990's, in the context of laser cooling. Atoms exposed to laser fields can exchange momentum with the photon field by radiating, and this behaviour can be exploited in order to cool a sample. Aside from the term that drives transitions and leads to radiation, the atom-laser interaction also contains a conservative term that acts as a potential for the atom's center of mass, and is proportional to the laser intensity. In 1991, Castin and Dalibard considered the effect of the latter term upon a laser cooling technique known as optical molasses [21]. They discovered that the periodic nature of the laser intensity leads to a Bloch band structure for the atoms' motion. A few years later, Jaksch and collaborators hit upon the idea of restricting their description to the lowest band, and showed that cold atoms in optical lattices are well-described by a Hubbard-like tight-binding Hamiltonian [33]. This brought about the realisation that optical lattices could be used to implement Feynman's quantum simulator idea [22], in this case as simulators of condensed matter systems [23]. Since then, optical lattices have been used to simulate existing condensed matter models [24, 25, 26], to realise novel phases of matter [27, 28, 29], and proposed as components in quantum technologies [30, 31].

As experimental systems and objects of theoretical study, optical lattices possess

many appealing features [23, 32]. One of the most obvious is their ability to trap both bosonic and fermionic particles, allowing us to study the behaviour of bosons in situations normally encountered only by fermions. Another is the high degree of control they offer over many parameters, such as tunneling amplitudes, particle-particle interaction strengths, lattice length, and particle number. One area of study which exploits all of these advantages is that of bosonic atoms in lattices with flat bands [16, 34, 35]. Flat bands support bases of strictly localised eigenstates, in the sense that the wavefunction vanishes exactly over the whole lattice, except for on a few neighbouring sites [36]. If the lowest-energy band is flat, then below a certain particle density ν_c the many-body ground state is a crystal composed of these localised states. The control offered by optical lattice systems allows us to investigate the transition away from this crystalline ground state, as the particle density is increased beyond ν_c: we can simply construct a lattice that is one unit cell too short to support the crystal, or add an extra atom on top of a preexisting crystal. Interestingly, this is a phenomenon where statistics and onsite interactions are likely to play an important role - indeed, as we will soon see, it is expected that the system above ν_c will behave qualitatively differently depending on whether the particles are allowed to overlap, as in the weakly-interacting bosonic case, or not, as in the fermionic and strongly-interacting bosonic cases. Therefore an optical lattice implementation is especially appealing [37], allowing us to study the system in all of these regimes. In the next chapter we will explore the physics of such a system at filling slightly above ν_c.

In order to discuss the physics of optical lattices, one must first understand the way in which light interacts with matter. This interaction has two facets; a dispersive part, where the light causes transitions between atomic energy levels, and a conservative part, taking the form of a coupling between the atomic dipole moment and the light field. Optical lattices rely on the latter facet, which gives rise to a potential landscape for the atomic center of mass degrees of freedom. To see how the field-dipole coupling comes about, let us begin with a description of a single, free atom; we then introduce a laser field into the picture, and consider the resulting

dynamics.

3.1 A single atom interacting with light

We now give a description of a single atom, and its behaviour in the presence of a laser field. When constructing a mathematical picture of a physical system, the first task is to choose the appropriate formalism. Since the ultimate goal is to understand optical lattices, which are low-speed, high-photon-number systems, there is no need to use quantum electrodynamics; rather, a Schrödinger equation description, with electromagnetism treated classically, is appropriate. The fine structure of the nucleus may also be neglected; we will treat it as a single particle. Thus, for our purposes, the degrees of freedom of a neutral atom consist of the nuclear coordinate, $\mathbf{r}_n$, and Z electronic coordinates, $\mathbf{r}_{e_i}$, Z being the nuclear charge or atomic number. These fundamental coordinates are not especially useful, however, so let us instead take the following set:

$$\mathbf{R} = \frac{1}{m_n + Zm_e}\left(m_n\mathbf{r}_n + m_e\sum_i \mathbf{r}_{e_i}\right), \tag{3.1}$$

$$\mathbf{r}_i = \mathbf{r}_n - \mathbf{r}_{e_i}, \tag{3.2}$$

where m_n is the mass of the nucleus, and m_e the mass of an electron. For convenience let us write down the gradient operators

$$\nabla_{r_{e_i}} = \frac{m_e}{m_n + Zm_e}\nabla_R - \nabla_{r_i}, \tag{3.3}$$

$$\nabla_{r_n} = \frac{m_n}{m_n + Zm_e}\nabla_R + \sum_j \nabla_{r_j}. \tag{3.4}$$

In terms of these coordinates, and in atomic units (which we use throughout this section), the atom's Hamiltonian is

$$H_{\text{atom}} = -\frac{\nabla_R^2}{2M} - \sum_{i=1}^{Z}\left(\frac{\nabla_{r_i}^2}{2\mu} - \frac{2Z}{|\mathbf{r}_i|} + \sum_{j>i}^{Z}\left[\frac{2}{|\mathbf{r}_i - \mathbf{r}_j|} + \frac{\nabla_{r_i}\cdot\nabla_{r_j}}{m_n}\right]\right), \tag{3.5}$$

where $M = m_n + Zm_e$ and $\mu = m_n m_e/(m_n + m_e)$. The last term in Eq. (3.5) - the "mass polarization" - is negligible due to the large magnitude of m_n/m_e. A key observation here is that the center of mass and relative coordinates are decoupled: we have $H = H_R + H_r$. Therefore the stationary Schrödinger equation has solutions of the form $\psi = \psi_R \otimes \psi_r$. Thus, the Hamiltonian gives an idea of the atom's low-energy behaviour: the center of mass will delocalise as a plane wave, and the Coulomb interaction between the nucleus and the electrons ensures that the relative degrees of freedom will occupy some bound state - or *level* - of H_r. For future use, let us denote these levels as $|\alpha\rangle$, so that $H_r|\alpha\rangle = E_\alpha|\alpha\rangle$.

Consider now the effect of exposing the above system to a laser field. The field enters the Hamiltonian via minimal coupling, $\nabla_{x_i} \to \nabla_{x_i} - e_i\mathbf{A}(\mathbf{x}_i, t)$, where e_i is the ith particle's charge. This has quite a complicated effect, and the resulting Hamiltonian requires simplification. To this end, it is convenient to employ the dipole approximation, which takes advantage of the fact that the bound states of H_r decay rapidly away from the center of mass $\mathbf{R}$, so that a slowly-varying gauge field is constant over their effective support, and one can replace $\mathbf{A}(\mathbf{x}_i, t) \to \mathbf{A}(\mathbf{R}, t)$. Under this approximation, we have

$$H = -\frac{\nabla_R^2}{2M} + \sum_{i=1}^{Z}\left(\frac{[-i\nabla_{r_i} - e\mathbf{A}(\mathbf{R},t)]^2}{2\mu} + \frac{2Z}{|\mathbf{r}_i|} - \sum_{j<i}^{Z}\frac{2}{|\mathbf{r}_i - \mathbf{r}_j|}\right), \tag{3.6}$$

where we note that the center of mass kinetic term is unaffected, as is clear from Eqs. (3.3) and (3.4): the contributions from the nucleus and from the electrons cancel one another. $\mathbf{R}$ *does* appear in the relative problem, however, so that the center of mass and orbital spaces become parametrically coupled. As we will see, this coupling results in an effective force for the center of mass degree of freedom.

The Hamiltonian as it stands is not particularly transparent, mainly due to the presence of the gauge field, which is difficult to interpret. It is possible, however, to eliminate $\mathbf{A}$ in favour of the more physical electric field $\mathbf{E}$. In order to do this, first note that

$$[-i\nabla_{r_i} - e\mathbf{A}(\mathbf{R},t)]^2\, e^{ie\mathbf{r}_i\cdot\mathbf{A}(\mathbf{R},t)}\psi(\mathbf{r}) = -e^{ie\mathbf{r}_i\cdot\mathbf{A}(\mathbf{R},t)}\psi(\mathbf{r}). \tag{3.7}$$

Since the goal is to eliminate $\mathbf{A}$, the above relation suggests the following transformation:

$$\psi(\mathbf{r}_1, ..., \mathbf{r}_Z, \mathbf{R}) \to \exp\left[ie\sum_{i=1}^{Z} \mathbf{r}_i \cdot \mathbf{A}(\mathbf{R}, t)\right] \psi(\mathbf{r}_1, ..., \mathbf{r}_Z, \mathbf{R}). \tag{3.8}$$

The gauge field, and therefore the transformation, depends on time, so the new Hamiltonian is obtained by plugging the above into the time dependent Schrödinger equation: upon doing this, we obtain

$$H = -\frac{\nabla_R^2}{2M} - \sum_{i=1}^{Z}\left(\frac{\nabla_{r_i}^2}{2\mu} - \frac{2Z}{|\mathbf{r}_i|} + \sum_{j<i}^{Z}\frac{2}{|\mathbf{r}_i - \mathbf{r}_j|} + e\mathbf{r}_i \cdot \mathbf{E}(\mathbf{R})\right), \tag{3.9}$$

$$= H_{\text{atom}} - e\sum_{i=1}^{Z} \mathbf{r}_i \cdot \mathbf{E}(\mathbf{R}). \tag{3.10}$$

where we have used the Coulomb gauge relation $\mathbf{E} = -\partial_t \mathbf{A}$. This is a nice result: upon the introduction of a laser field, the free atomic Hamiltonian is preserved, save for the addition of a single term which couples the electrons to the electric field in a simple way [38]. The optical potential that we are seeking for is nothing more than the energy shift exerted upon the atomic levels by this coupling. To see this, it is helpful to consider the action of H in the basis of levels, $\{|\alpha\rangle\}$. The action of H_{atom} in this basis is clear, so let us concentrate on the extra term, which, if one chooses the standard complex representation for the laser field, can be written as

$$V = e\sum_{\alpha,\beta}\sum_{i=1}^{Z} (\boldsymbol{\mathcal{E}}(\mathbf{R})e^{-i\omega t} + \boldsymbol{\mathcal{E}}^*(\mathbf{R})e^{i\omega t}) \cdot \langle\alpha|\mathbf{r}_i|\beta\rangle \ |\alpha\rangle\langle\beta|. \tag{3.11}$$

Although the above potential seems to couple all the atom's levels together, complicating the dynamics considerably, it can in fact represent a significant simplification, yielding behaviour that is more easily understood than that of the free atomic system. In particular, if the frequency ω is close to that of some transition, $\omega \approx (E_\alpha - E_{\alpha'})$, then the coupled system can be modeled solely in terms of the states $|\alpha\rangle$ and $|\alpha'\rangle$; it becomes effectively a two-level system. This is most easily seen by transforming to the interaction picture via the unitary operator

$U(t) = \exp(-it\sum_\alpha E_\alpha|\alpha\rangle\langle\alpha|)$, whereby the potential V becomes

$$V = \sum_{\alpha\beta}\sum_{i=1}^{Z}\left(e^{i(E_\alpha - E_\beta - \omega)t}\boldsymbol{\mathcal{E}}(\mathbf{R}) + e^{i(E_\alpha - E_\beta + \omega)t}\boldsymbol{\mathcal{E}}^*(\mathbf{R})\right)\cdot\langle\alpha|\mathbf{r}_i|\beta\rangle\ |\alpha\rangle\langle\beta|. \tag{3.12}$$

In this picture, one sees that every transition $|\beta\rangle \to |\alpha\rangle$ comes with a temporally oscillating coefficient. If one is interested in the dynamics on timescales similar to that of the slowest oscillation, and if the other oscillations are significantly fast by comparison, then one may ignore all but the most slowly-oscillating terms: the others will average out to zero over the relevant timescale. Clearly, the slowest-oscillating terms are associated with the transition where $|E_\alpha - E_\beta|$ is closest to ω. Thus, one may drop all other terms and regard the potential as driving a transition between two levels only - call them $|g\rangle$ and $|e\rangle$. If a free atom is prepared in either state, or some superposition of the two, and the laser field is subsequently introduced, the atom will behave as a two-level system. In that case, returning to the Schrödinger picture, then transforming once again to a time-dependent frame - this time to one that rotates along with the laser field, $\psi \to e^{i\omega t(|e\rangle\langle e| - |g\rangle\langle g|)}\psi$ - we have

$$H = -\frac{\nabla_R^2}{2m} - \frac{\Delta}{2}|e\rangle\langle e| + \left[\Omega(\mathbf{R})e^{-i\omega t}|e\rangle\langle g| + h.c.\right], \tag{3.13}$$

where we have defined the Rabi frequency $\Omega(\mathbf{R}) = \sum_i 2\boldsymbol{\mathcal{E}}(\mathbf{R})\cdot\langle g|\mathbf{r}_i|e\rangle$, the detuning $\Delta = E_e - \omega$, and have set the ground state energy to zero. For a sufficiently weak electric field, the energy shift due to the last term can be calculated perturbatively. To second order, one obtains

$$\Delta E_{g,e} \propto \pm\frac{\Omega^2(\mathbf{R})}{\Delta}, \tag{3.14}$$

where the plus sign corresponds to the shift for $|g\rangle$. Thus, an atom in the perturbed ground state[1] feels a center-of-mass-dependent potential $U(\mathbf{R}) = \frac{\Omega^2(\mathbf{R})}{\Delta}$ due to the light field. For $\Delta > 0$, such atoms will seek regions of low field intensity, and the opposite for $\Delta < 0$. This is the effect that allows for the creation of an optical lattice

[1] We assume that the atoms remain in a particular perturbed eigenstate throughout the interaction. This is reasonable for large values of Δ.

[32].

3.2 Many atoms interacting with each other

We have seen how a laser field may induce an optical potential for a single atom. Optical lattices are interesting because of their ability to hold many atoms, however. So, as well as the interaction between atoms and light, it is important to understand the behaviour of a group of atoms that interact with one another. The atoms occupying optical lattice systems are usually initially Bose-condensed, and so it is this phase in particular that we must understand.

To begin with, consider the potential between a pair of atoms, which, although extremely complicated in detail, is often dominated by the dipole-dipole and short-range repulsive forces, and hence well-approximated by the Lennard-Jones potential, $V(r) \propto \sigma_{12}/r^{12} - \sigma_6/r^6$. This potential supports bound states, so that the ground state of a many-atom system is a bound cluster. Thus, an ensemble of atoms, sufficiently cooled, might be expected to solidify; indeed, at low temperatures, ensembles interacting via the Lennard-Jones potential are solid at thermodynamic equilibrium. There exists, however, a metastable state above the solid phase: the Bose-Einstein condensate (BEC). In a BEC, the atoms are not bound to one another. Rather, the main bulk of the many-body wavefunction is concentrated on configurations where the atoms are well-separated. Despite being thermodynamically unfavourable, this gaseous phase can persist for a significant amount of time if the gas is sufficiently dilute. To see why, note that the requirements of energy and momentum conservation forbid a pair of initially-unbound atoms from binding by themselves. A third particle is required, in order to convert the kinetic energy of the pair into binding energy. In other words, molecule formation requires three-body collisions. In a highly dilute gas such collisions are very rare, so that the gas is metastable.

Given that three-body processes are rare, and since two-body collisions cannot lead to bound states, it is clear that two-body scattering events are the most important interaction processes in the BEC phase. Therefore, rather than using a hard-to-treat interaction like the Lennard-Jones potential, it seems sensible to

choose a simpler interaction. As long as the simpler interaction reproduces the correct two-body scattering properties, it will be suitable for use as an effective potential between the particles in a Bose-condensed gas. Moreover, as was shown in the previous chapter, two-body scattering properties at low energies are determined by a single parameter, the scattering length. Therefore one may choose an effective interaction that also depends only on a single parameter. We opt for

$$V(r) = g\delta(\mathbf{r}). \tag{3.15}$$

For simplicity, let us work with identical bosons and calculate the scattering properties due to this potential in the principal value formalism. From the Lippmann-Schwinger equation 2.47 for $\mathcal{T}$, we have

$$\langle \mathbf{p}'|\mathcal{T}(E_p)|\mathbf{p}\rangle = \frac{g}{(2\pi)^3} + \frac{g}{(2\pi)^3}\mathcal{P}\int d^3q \frac{\langle \mathbf{q}|\mathcal{T}(E_p)|\mathbf{p}\rangle}{E_p - E_q}. \tag{3.16}$$

One immediately notices that $\langle \mathbf{p}'|\mathcal{T}(E_p)|\mathbf{p}\rangle$ is independent of $\mathbf{p}'$; therefore, when E is symmetric about E_p (as in the low-energy limit), the principal value integral vanishes, and we see that

$$\langle \mathbf{p}'|\mathcal{T}(E_p)|\mathbf{p}\rangle = \frac{g}{(2\pi)^3}. \tag{3.17}$$

Using this in Eq. (2.36) and taking the position-space representation yields

$$\psi_{\mathbf{p}}(\mathbf{x}) = \frac{\cos(\mathbf{p}\cdot\mathbf{x})}{(2\pi)^{3/2}} + \frac{g}{(2\pi)^6}\mathcal{P}\int d^3q \frac{e^{i\mathbf{q}\cdot\mathbf{x}}}{E_p - E_q} \tag{3.18}$$

$$\Rightarrow \psi_{\mathbf{p}}(0) = \frac{1}{(2\pi)^{3/2}} \tag{3.19}$$

On the other hand, from Eq. (2.17) one sees that

$$\psi_{\mathbf{p}}(\mathbf{x}) = \frac{\cos(\mathbf{p}\cdot\mathbf{x})}{(2\pi)^{3/2}} - \frac{mg}{4\pi\hbar^2}\frac{e^{ipr}}{r}\psi_{\mathbf{p}}(0). \tag{3.20}$$

where we have used the reduced mass, since we are considering the relative coordinate problem. Thus, from Eq. (2.19) and the definition of the scattering length a,

we find:

$$a = \frac{mg}{4\pi\hbar^2}. \tag{3.21}$$

The coupling strength g should be chosen so that a is the actual scattering length for the particles under consideration - this can be measured experimentally, or calculated numerically using a realistic interaction. Thus, a dilute ultracold atomic gas is well described by the (bare) Hamiltonian

$$H = \sum_i \left[\frac{p_i^2}{2m} + g \sum_{j>i} \delta(\mathbf{x}_i - \mathbf{x}_j) \right], \tag{3.22}$$

where $\mathbf{x}_i$ is the center of mass coordinate of the ith atom.

3.3 Optical lattices and the Bose Hubbard model

In this section, the basic model for ultracold atoms in optical lattices - the Bose-Hubbard model - is developed. Upon introducing a BEC to a laser field far detuned from any of the constituent atoms' transitions, the center of mass degrees of freedom of the atoms will experience the energy shift (3.14). Suppose that the laser intensity is such that the energy shift is given by a periodic function $V_L(\mathbf{x})$. The Hamiltonian for a BEC exposed to such a laser field, in second-quantised form, is

$$\begin{aligned} H = \int d^3x\, \psi^\dagger(\mathbf{x}) \left(\frac{\hbar^2}{2m}\nabla^2 + V_L(\mathbf{x}) \right) \psi(\mathbf{x}) \\ + \frac{g}{2} \int d^3x\, \psi^\dagger(\mathbf{x})\psi^\dagger(\mathbf{x})\psi(\mathbf{x})\psi(\mathbf{x}), \end{aligned} \tag{3.23}$$

where we have simply added the laser-induced energy shift to the Hamiltonian (3.22) and second-quantised it. $\psi^\dagger(\mathbf{x})$ creates an atom at position $\mathbf{x}$ and satisfies $[\psi(\mathbf{x}), \psi^\dagger(\mathbf{x}')] = \delta(\mathbf{x} - \mathbf{x}')$. In treating this model, it will once again be useful to consider low-energy physics. In the previous chapter, such a restriction was facilitated by the quantised angular momentum of scattering particles, and the present model contains a similarly natural energy barrier: the energy difference between the periodic potential's lowest Bloch band and the higher bands. According to Bloch's theorem, since the potential $V_L(\mathbf{x})$ is periodic, the single-particle eigenstates of the

Hamiltonian (3.23) can be written as

$$\phi_{\mathbf{k}}^{(j)}(\mathbf{x}) = e^{i\mathbf{k}\cdot\mathbf{x}} u_{\mathbf{k}}^{(j)}(\mathbf{x}), \tag{3.24}$$

with $\mathbf{k}$ - referred to as the quasimomentum - in the first Brillouin zone. The $u_{\mathbf{k}}^{(j)}(\mathbf{x})$ must have the same periodicity as the lattice. To get an idea of what these functions look like, let us consider a one dimensional system, and use Bloch's form for the eigenfunctions in the single-particle stationary Schrödinger equation. Then, one sees that the $u_k^{(j)}(x)$ must satisfy

$$\left(\frac{(\hat{p} + \hbar k)^2}{2m} + V_L(x) \right) u_k^{(j)}(x) = E^{(j)}(k) u_k^{(j)}(x). \tag{3.25}$$

If $V_L(x)$ is a periodic array of wells, $V_L(x + d) = V_L(x)$, with d the lattice spacing, as in an optical lattice, the equation need only be solved for a single well, with periodic boundary conditions imposed. In the case where $k = 0$, then, it reduces to the usual Schrödinger equation over a single well, which will support a number of bound states. Thus, $u_k^{(j)}$ is related by a continuous transformation, parameterised by k, to the jth bound state of the well. As k increases, the $u_k^{(j)}$ tend to localise more strongly within the well; this behaviour is illustrated in Fig. 3.1. Similarly, the function $E^{(j)}(k)$ - referred to as the band's dispersion - must be equal to the energy of the jth bound state at $k = 0$. The extent to which bands are separated energetically is thus influenced by the energy difference between the bound states - the *band gap*. Since with optical lattices one can control the depth of the wells, and hence the energy gap between the bound states, one can always engineer the system so that the lowest band is well-separated from the upper bands. In that case, at low densities and low temperatures, all the particles in the lattice will occupy the lowest band, and we may restrict the Hilbert space accordingly.

In order to see what the Hamiltonian looks like upon restricting $\mathcal{H}$ to the lowest band, it is convenient to introduce localised functions, known as Wannier functions, taking the form

$$w_{\mathbf{R}}^{(j)}(\mathbf{x}) = \frac{1}{\sqrt{N}} \sum_{\mathbf{k} \in \mathrm{BZ}_1} e^{-i\mathbf{k}\cdot\mathbf{R}} \phi_{\mathbf{k}}^{(j)}(\mathbf{x}), \tag{3.26}$$

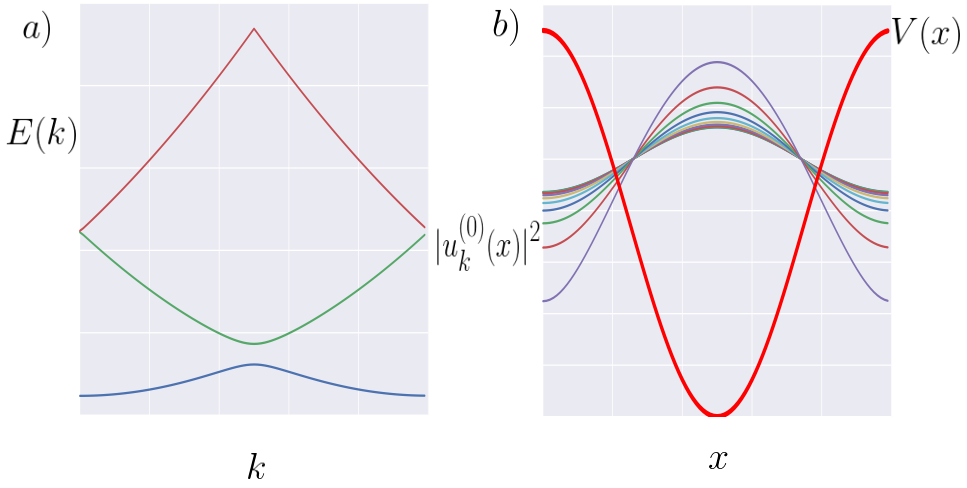

Figure 3.1: a) The three lowest Bloch bands for a potential $V = V_0 \sin^2(x)$. As V_0 increases, so does the gap between the bands. b) The functions $u_k^{(0)}$ at various values of k, for a single period of the same potential (plotted in red). The better-localised state have larger values of k.

where $\mathbf{R}$ is a lattice vector, and N is the number of lattice sites in the system. The convenience of these functions lies in the fact that the set $\{w^{(j)}\}$ forms an orthonormal basis for the jth band, and that the $w_{\mathbf{R}}$ are localised around $\mathbf{R}$ [39]; thus, the $w_{\mathbf{R}}^{(0)}$ provide a well-localised basis for the lowest band, in terms of which we can construct a projected Hamiltonian. To carry out the projection, note that the operator $\psi^\dagger(\mathbf{x})$ maps the vacuum $|0\rangle$ to a state which we may write in first quantised notation as $|\mathbf{x}\rangle$. The projection of $\psi^\dagger(\mathbf{x})$ onto the lowest band must therefore map $|0\rangle$ to the projection of $|\mathbf{x}\rangle$ onto the lowest band. Since the overlap between the Wannier state $\int d^3x w_{\mathbf{R}}^{(j)}(\mathbf{x})|\mathbf{x}\rangle$ and $|\mathbf{x}\rangle$ is just $w_{\mathbf{R}}^{(j)}(\mathbf{x})$, it is clear that the projection can be implemented as

$$\psi(\mathbf{x}) \to \sum_i w_{\mathbf{R}_i}^{(0)*}(\mathbf{x}) b_i, \tag{3.27}$$

where b_i is an operator creating a Wannier state at $\mathbf{R}_i$. Plugging the projected operators into the Hamiltonian (3.23), we obtain the Bose-Hubbard Hamiltonian

[33],

$$H = \sum_{\langle i,j \rangle} t_{i,j} b_i^\dagger b_j + \frac{U}{2} \sum_i \hat{n}_i(\hat{n}_i - 1), \tag{3.28}$$

where $\langle i, j \rangle$ denotes a pair of adjacent lattice sites. Dropping the band index, we have

$$U \approx g \int d^3x |w_{\mathbf{R}_i}(\mathbf{x})|^4, \tag{3.29}$$

representing the onsite repulsion between two atoms[2] (assumed to be the same at all sites, although one can easily add a site index if necessary), and

$$t_{i.j} = -\int d^3x w^*_{\mathbf{R}_i}(\mathbf{x}) \left(\frac{p^2}{2m} + V_L(\mathbf{x}) \right) w_{\mathbf{R}_j}(\mathbf{x}), \tag{3.30}$$

which gives the rate of tunneling between the sites i and j. Since $t_{i,j}$ depends on the distance between the lattice wells, and on their depth, it is tunable. Also, U depends on g, which in turn depends on the scattering length of the atoms comprising the BEC. Since this is tunable via magnetic Feshbach resonance [40], U is tunable. The fact that optical lattices provide experimental control over the Bose-Hubbard model's two key parameter sets (tunneling and onsite interactions) makes them ideal for testing condensed matter models, and for experimentally realising novel phases of matter.

3.4 Positive tunneling through periodic driving

The next chapter will be concerned with an exotic ground state, found in a lattice system where the lowest band is flat (i.e, independent of quasimomentum). The system in question has two bands, only one of which can become flat. Whether this is the upper or the lower band depends on the sign of the tunneling; if t_{ij} is negative, for instance, only the upper band can become flat. This adds a complication, since the t_{ij} are indeed negative for standard optical lattices, and the lattice that we wish to work with is no exception [37]. Thus, we require a method for tuning the hopping parameters through to positive values. Fortunately, periodic driving

[2] A technique for calculating this quantity non-perturbatively is found in [41]

provides just such a method: adding a fast periodic term to a Hamiltonian gives rise to dynamics that are close to the dynamics of the undriven system, but with the original parameters modified in a way that depends on the driving. This can be exploited in order to obtain the required hopping sign, by rapidly moving the lattice along a small elliptical orbit [42]. We now briefly sketch the idea, following the treatment of [43].

In order to see that a fast periodic driving leads to a dressing of the static system's parameters, it is convenient to split the time evolution into inter- and intra-period parts. Interperiod evolution moves the system forward in time by one period (denoted T), and its corresponding evolution operator can be regarded as time-independent, given a choice of initial time. The intraperiod evolution then accounts for the remaining dynamics, or micromotion, and is generated by a time-dependent operator. If the driving is sufficiently fast, the dynamics on the driving timescale and on the undriven timescale decouple. In that case, the interperiod operator takes the form of a renormalised undriven evolution operator. The intraperiod operator rapidly modulates this behaviour and, if one is interested only in dynamics on the undriven timescale, may be time-averaged away.

Let us see how this works in more detail. To begin with, note that the time evolution operator for a driven system takes the form

$$U(t_2, t_1) = \mathcal{T}\exp\left(-\frac{i}{\hbar}\int_{t_1}^{t_2} dt H(t)\right) \tag{3.31}$$

where $\mathcal{T}$ denotes time ordering. Now, consider the operator $U(t_1 + T, t_1)$ taking the system forward in time by one period, starting from time t_1. For a fixed t_1, this operator is time independent, and, since it is unitary, it has a Hermitian generator, which we call the Floquet Hamiltonian $H_F^{(t_1)}$. Then,

$$U(t_1 + T, t_1) = e^{-\frac{i}{\hbar}H_F^{(t_1)}T}. \tag{3.32}$$

From the periodicity, it is evident that

$$U(t_1 + nT, t_1) = e^{-\frac{i}{\hbar}H_F^{(t_1)}nT}. \tag{3.33}$$

The goal is now to separate fast and slow dynamics, i.e, to consider the evolution generated by H_F separately from that occurring on short, intraperiod timescales. In order to facilitate this separation, suppose that there are n periods between t_1 and t_2, so that $t_2 - t_1 = nT + \tau$, with $0 \leq \tau < T$, and imagine the evolution as a three step process. In the first step, the system evolves from t_1 to t_2 under H_F. Unless $\tau = 0$, this evolution clearly will not yield the physical state at time t_2. However, the trajectory generated by H_F intersects the physical trajectory at the time $t_2 - \tau$. Therefore, as the second step, let the system evolve backwards in time under H_F, up to $t_2 - \tau$. The physical state at time t_2 may then be reached in the final step by evolving under the full Hamiltonian from $t_2 - \tau$ to t_2. Mathematically, this argument reads

$$U(t_2, t_1) = U(t_2, t_2 - \tau)\, e^{\frac{i}{\hbar}H_F^{(t_1)}\tau}\, e^{-\frac{i}{\hbar}H_F^{(t_1)}(t_2 - t_1)}, \tag{3.34}$$

$$\equiv e^{-\frac{i}{\hbar}K^{(t_2)}\tau}\, e^{-\frac{i}{\hbar}H_F^{(t_1)}(t_2 - t_1)}. \tag{3.35}$$

Thus, we have separated the evolution operator into a time independent part, generated by $H_F^{(t_1)}$ and governing interperiod evolution, and a time dependent part, generated by $K^{(t_2)}$ and governing the evolution on intraperiod timescales, which may be averaged over. This is the form of time evolution employed in works on periodic driving in optical lattices [42, 44, 45, 46].

In order to see that H_F does indeed behave like the undriven Hamiltonian with renormalised parameters, a perturbative approach may be used. From Eqn's (3.31) and (3.32), one sees that

$$H_F^{(t_1)} = \frac{i}{\hbar T} \log \left[\mathcal{T} \exp \left(-\frac{i}{\hbar} \int_{t_1}^{t_1+T} dt\, H(t) \right) \right]. \tag{3.36}$$

Thus, $H_F^{(t_1)}$ has a Baker-Campbell-Hausdorff expansion, or Dyson series, the nth

term of which involves an integral over a region whose size is proportional to T^n. If $H(t)$ is independent of T and the driving frequency ω is high, therefore, it is reasonable to replace the Floquet Hamiltonian by the first term in its Dyson series, which is nothing but the time average of the full, time-dependent Hamiltonian over a period. In many cases, however, $H(t)$ does depend on T, since the driving amplitude often scales with ω. In order to deal with such situations, one may transform to a time-dependent frame which co-rotates with the driving. Specifically, suppose that the time-dependent Hamiltonian takes the form

$$H(t) = H_0 + \omega^\alpha \lambda(t) H_1. \tag{3.37}$$

Then, it is helpful to transform to a rotating frame as

$$|\psi_r(t)\rangle = \exp\left(i\omega^\alpha \int_{t_1}^{t} dt' \lambda(t') H_1\right) |\psi(t)\rangle \equiv V^\dagger(t)|\psi(t)\rangle. \tag{3.38}$$

The Hamiltonian becomes

$$H_r(t) = V^\dagger(t) H_0 V(t). \tag{3.39}$$

The Dyson series for the Floquet Hamiltonian in this frame is well behaved in the $T \to 0$ limit; it is just the time average $\frac{1}{T}\int_0^T dt H_r(t)$.

Let us now particularise to the Bose-Hubbard model, to which we add a periodic driving term modulating the onsite energies by functions $v_i(t) = \mathbf{r}_i \cdot \mathbf{F}$, where $\mathbf{F} = \omega^2 \left(F_c \mathbf{e}_c \cos(\omega t) + F_s \mathbf{e}_s \sin(\omega t)\right)$. $F_{c,s}$ are driving amplitudes, $\mathbf{e}_{c,s}$ are orthogonal vectors, and $\mathbf{r}_i$ are the positions of the lattice sites. Such a modification is attainable experimentally, by methods described in [47, 48]. We have

$$H(t) = \sum_{\langle i,j \rangle} t_{i,j} b_i^\dagger b_j + \frac{U}{2} \sum_i \hat{n}_i(\hat{n}_i - 1) + \sum_i v_i(t)\hat{n}_i. \tag{3.40}$$

Transforming to a rotating frame as described above and taking the high-frequency

limit $T \to 0$, we find the Floquet Hamiltonian (with $t_1 = 0$)

$$H_F = \sum_{\langle i,j \rangle} \tilde{t}_{i,j} b_i^\dagger b_j + \frac{U}{2} \sum_i \hat{n}_i(\hat{n}_i - 1) \tag{3.41}$$

where

$$\tilde{t}_{i,j} = t_{i,j} J_0\left(\alpha_{i,j}\right) \tag{3.42}$$

$$\alpha_{i,j} = \sqrt{\sum_{\mu=e,s} \left[F_\mu \mathbf{e}_\mu \cdot (\mathbf{r}_i - \mathbf{r}_j)\right]^2}, \tag{3.43}$$

with J_0 the zero-order Bessel function [42]. Thus, by modifying the angle of oscillations or the oscillation amplitude, one can tune the effective hopping through to positive values. As an aside, it is interesting to note that $\alpha_{i,j}$ can be tuned to a zero of J_0, which will suppress tunneling and result in *dynamical localisation*.

Chapter 4

Flat band Bose-Hubbard system above critical filling

In this chapter we study a Bose-Hubbard model whose lowest Bloch band is flat, i.e., has constant energy. The irrelevance of kinetic energy for physics in flat bands allows for the emergence of strongly correlated phases, and it is this property that has attracted the strongest theoretical interest historically [1]. For instance, flat bands played a key role in the early understanding of ferromagnetism, where they provided an ideal setting for the study of magnetic interactions without the distraction of kinetic behaviour, allowing for the proof of important theoretical results [50, 51, 52]. Physicists studying another strongly correlated phase, the superconductor, have also found use for flat-banded models [53], and the analogy between flat bands and Landau levels allows for the use of optical lattice systems as experimental testing grounds for quantum Hall physics [54, 55, 56].

Flat bands have an intimate connection with localisation: they admit bases of localised single particle eigenfunctions, allowing for the formation of Wigner-crystal-like many-body eigenstates. In this chapter, we investigate such a crystalline state, and in particular its behaviour when an extra particle is introduced on top of the crystal, in the context of an experimentally realisable optical lattice system [37]. The lattice that we consider - the sawtooth chain - has a flat lower band and a dispersive

[1] Note that this is not the only interesting feature of flat banded-systems. They also have highly unusual few-body scattering properties, a fact that we will touch upon later in this thesis, and that is explored more fully in [49].

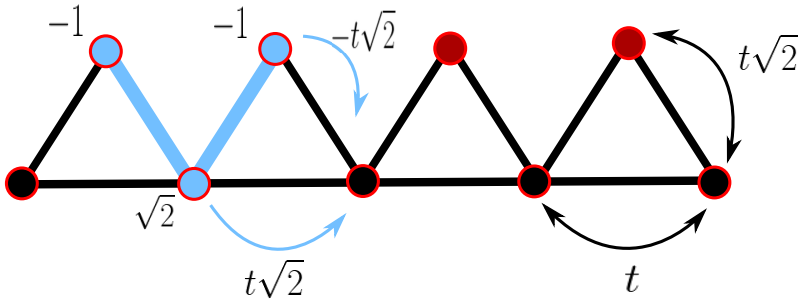

Figure 4.1: The sawtooth lattice, occupied by a single localised state. The light blue sites are occupied, with the weights appearing next to them. On the right of the figure, the tunneling amplitudes leading to a flat band are shown. The interference effect characteristic of flat bands is illustrated with blue arrows. The sites adjacent to the localised state receive a total weight of zero from hopping.

upper band, so that the relevant behaviour may be brought about experimentally by cooling the system to its ground state. We find that the extra particle causes a defect in the crystal, which inherits the dispersive character of the upper band and moves throughout the otherwise intact crystalline medium.

4.1 Flat bands and localised states

A flat band is a Bloch band in which energy is constant, that is, independent of quasimomentum. One of the more striking features characteristic of flat bands is their connection with localised states: it seems that every flat band supports a basis of exactly local eigenstates. Surprisingly, there is no known theorem asserting that this must be so [57] but the present author is unable to find a single example of a flat band which does not have this property. Given the lack of a general theorem, we give a few heuristic comments about the relationship between flat bands and localised states. One can argue in two directions: the existence of the localised states can be thought of as a consequence of the flatness of the band, or vice versa. Arguing in the first direction, recall that the single-particle eigenstates of lattice models are Bloch waves, which are analogous to plane waves in the continuum. In the continuum one is able to construct almost any position-space function by superposing plane waves, and it is not hugely surprising that enough of this freedom survives on the lattice so that one is always able to construct localised states from Bloch waves belonging to the same band. If the kinetic term is degenerate with respect to quasimomentum,

as in a flat band, these localised states will be eigenstates. Arguing in the other direction, one could claim that flat-banded lattices are precisely those on which tunnelling is frustrated by destructive interference. This is best illustrated with an example. Fig. 4.1 shows a localised state together with the hopping amplitudes on the flat-banded sawtooth lattice. Notice how the contribution received by the sites surrounding the V-state from hopping is zero, because of a cancellation between contributions from different V-state sites. This kind of destructive interference is a general feature of localised flat band states, and means that the localised state behaves like a particle of zero group velocity or of infinite mass, or in other words, a particle with a constant dispersion relation.

This link between localised states and flat bands leads to a peculiar type of low energy behaviour in systems whose lowest band is flat. Consider a lattice of length L with a flat lowest band, and let the associated localised states occupy l sites each. Also, suppose that the lattice contains $N < L/l$ particles. Then, for positive interactions $U > 0$, it is easy to see what the ground state is. The system can avoid the energetic penalty for particle-particle overlap by forming a crystal of non-overlapping localised flat band states; since each of these states is itself an eigenstate, and since they do not overlap, such a crystal is also an eigenstate. Also, it must be the ground state. The interactions are positive, hence there is no other arrangement possessing a lower energy.

4.2 The sawtooth chain: band structure and ground state below critical filling

We choose to work with perhaps the simplest lattice that admits a flat lowest band, the one-dimensional sawtooth chain. In the following we derive its band structure. There are two independent hopping amplitudes in the model: hopping between between two lower sites, which we parameterise by the quantity t, and hopping between upper and lower sites, parameterised by $t\alpha$ (see Fig. 4.1). Thus, the t_{ij} in

the Hamiltonian (3.28) for this model are

$$t_{2i,j} = t(\delta_{|2i-j|,2} + \alpha\delta_{|2i-j|,1}), \tag{4.1}$$

$$t_{2i+1,j} = t\,\alpha\,\delta_{|2i+1-j|,1}. \tag{4.2}$$

To find the band structure, we must solve the single-particle stationary Schrödinger equation $H\psi = E\psi$. It is convenient to use the first quantised form in order to do this. We have

$$\sum_{\mu=\pm1} t\left(\alpha\,\psi(j+\mu) + \frac{(1+(-1)^j)}{2}\psi(j+2\mu)\right) = E\psi(j). \tag{4.3}$$

We now employ Bloch's theorem, writing the wavefunction as $\psi_k^{(n)}(j) = e^{ikj}\phi^{(n)}(j)$. Since there are two sites per unit cell, n is either 0 or 1, and the $\phi^{(n)}(j)$ take only two values (since $\phi^{(n)}(j+2) = \phi^{(n)}(j)$). Therefore without loss of generality we solve the above for $j = 0$ and $j = 1$, obtaining

$$t\left(2\alpha\cos(k)\phi^{(n)}(1) + 2\cos(2k)\phi^{(n)}(0)\right) = E^{(n)}(k)\phi^{(n)}(0), \tag{4.4}$$

$$2t\,\alpha\cos(k)\phi^{(n)}(0) = E^{(n)}(k)\phi^{(n)}(1), \tag{4.5}$$

where k is in units of inverse lattice spacing. Solving for the energy, we have

$$E_k^{(\pm)} = t\left(\cos(2k) \pm \sqrt{\cos^2(2k) + 4\alpha^2\cos^2(k)}\right) \tag{4.6}$$

We must tune $\alpha = \sqrt{2}$ to obtain a flat band. Then,

$$E^+ = 2t(1+\cos(2k)), \tag{4.7}$$

$$E^- = -2t. \tag{4.8}$$

Thus, in order for the flat band to have the lower energy of the two, we require $t > 0$. Positive hopping parameters do not occur naturally in optical lattices; hence, for an experimental realisation, the periodic driving technique discussed in the previous chapter must be employed.

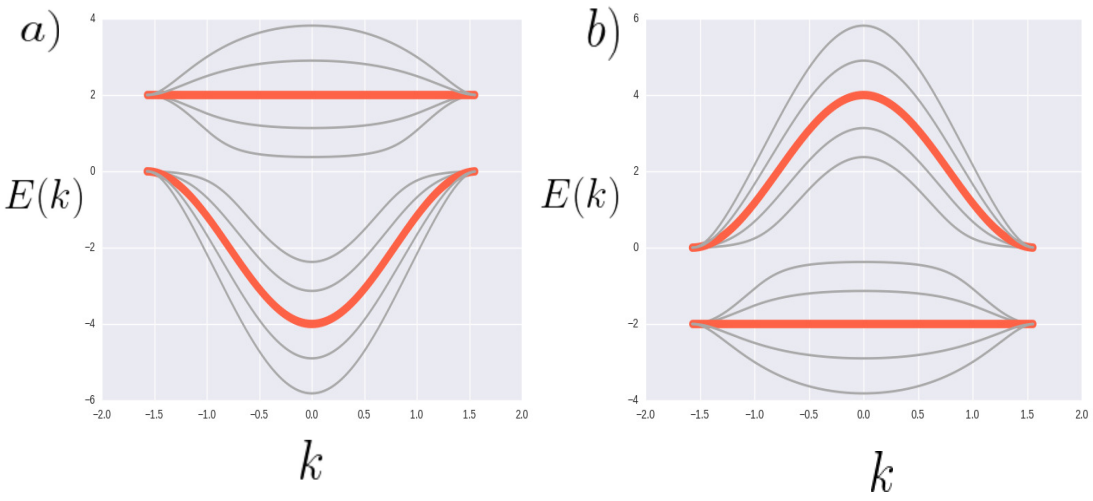

Figure 4.2: The band structure for the sawtooth chain for a) negative and b) positive hopping amplitues. The dispersion is plotted for various ratios of the two hopping parameters, with the flat band at ratio $\alpha = \sqrt{2}$ (see text) highlighted in red. Here, k is in units of $1/a$, with a the lattice spacing (set to unity in the text)

The localised states associated with the flat band are

$$V_i^\dagger|0\rangle \equiv \left(\sqrt{2}b_{2i}^\dagger - b_{2i+1}^\dagger - b_{2i-1}^\dagger\right)|0\rangle. \tag{4.9}$$

Clearly, at most $L/4$ of these states can fit on the lattice without overlapping; thus, the critical density or *critical filling* is $\nu_c = 1/4$. Below this value of ν, the degenerate ground states take the form

$$|\psi_0^{(N)}\rangle = \prod_{i\in\mathcal{S}} V_i^\dagger|0\rangle \tag{4.10}$$

where $\mathcal{S} = \{i_1, i_2, ..., i_N : |i_m - i_n| > 1\,\forall m, n\}$, N being the number of particles. One can verify that

$$H|\psi_0^{(N)}\rangle = -2Nt|\psi_0^{(N)}\rangle. \tag{4.11}$$

The ground state energy below critical filling is therefore $E_0(N) = -2Nt$.

4.3 Above critical filling

While the low-energy behaviour of our system is simple below the critical filling factor ν_c, it is not at all clear what should be expected when the system contains more particles than the crystal of localised flat band states can accommodate. The

rest of this chapter will be concerned with understanding this regime. In particular, we are interested in how the system behaves when it contains a single particle more than the critical number.

To begin with, note that one can expect two different classes of behaviour, depending on the magnitude of U as compared with that of the band gap Δ, which sets the energy scale for interactions. Interaction strengths small compared with Δ will give rise to qualitatively different behaviour from the case where $U > \Delta$. The key difference between these two situations is the extent to which the upper band, and hence kinetic energy, is expected to contribute to the low-energy behaviour. If $U \ll \Delta$, overlap between particles is less energetically costly than exciting a particle to the upper band. Hence, at slightly above critical filling, one expects all of the particles to remain in the flat band, minimising overlap under this constraint. Beyond confining the particles to the flat band, then, kinetic energy plays no role in weakly-coupled systems. If $U > \Delta$, on the other hand, it will be favourable for particles to avoid overlap, even at the cost of exciting transitions to the upper band. Therefore dispersive behaviour should play a role at any filling $> \nu_c$ in the strong-coupling case. The weakly-interacting case has been treated by Altman and Huber [16]; therefore, our interest will be focused on a strongly-interacting system.

Our first task is to find a method that will allow us to investigate the system properly. A perturbative approach is impossible: the strongly-correlated nature of the system means that there is no "non-interacting" state that can be used as a starting point for perturbation theory. Altman and Huber's strategy of projecting onto the flat band is also inappropriate in the strongly-interacting case, since, as we have just argued, the upper band is expected to contribute once critical filling is exceeded - in fact, such a projection will result in states with energies of order U. Thus, we opt for a variational approach, using the Ritz method, which is described in Appendix A.

4.3.1 Ground state energy scaling

In order to apply the Ritz method we must guess a set of states that span the low-energy subspace. To this end, we now attempt to obtain some insight into the structure of the ground state at one particle above critical filling. Note that there are two qualitatively different possibilities: upon the addition of an extra particle to the critically-filled lattice, either the crystalline structure will be completely destroyed and a different configuration will take its place, or the crystal will be mostly preserved, with the disruption caused by the extra particle confined to a few cells (the confined disruption may delocalise, of course, but in this case it would do so through a medium of preserved localised flat band states). We can determine which of these two behaviours is realised by investigating how the ground state energy scales with system size. In particular, as we now argue, it is relatively clear what the ground state energy scaling should look like in the second scenario.

Suppose that adding a single particle to a critically filled lattice disrupts a number of the crystal's unit cells, N_D. Suppose further that N_D is a constant, independent of the lattice length L - in other words, no matter whether the lattice is twenty or two thousand sites long, adding an extra particle on top of the crystal disrupts exactly N_D of its unit cells. The defect caused by the extra particle would have an energy - call it C - which would also be independent of the lattice length (or, equivalently since we are always considering critically filled lattices, of the particle number). The total energy of the system, after the addition of the extra particle, would thus be $C-(N-N_D)2t$ (recall that the localised flat band states have energy $-2t$). Let us therefore define

$$C(N) \equiv E_0(N) + (N - N_D)2t, \tag{4.12}$$

where $E_0(N)$ is the N-particle ground state energy. If $C(N)$ can be shown to be independent of N, it is likely that the number of unit cells disrupted by the extra particle does not depend on the lattice size. In other words, the extra particle cause a localised defect in the crystal, leaving the rest intact. To check whether this is so, we

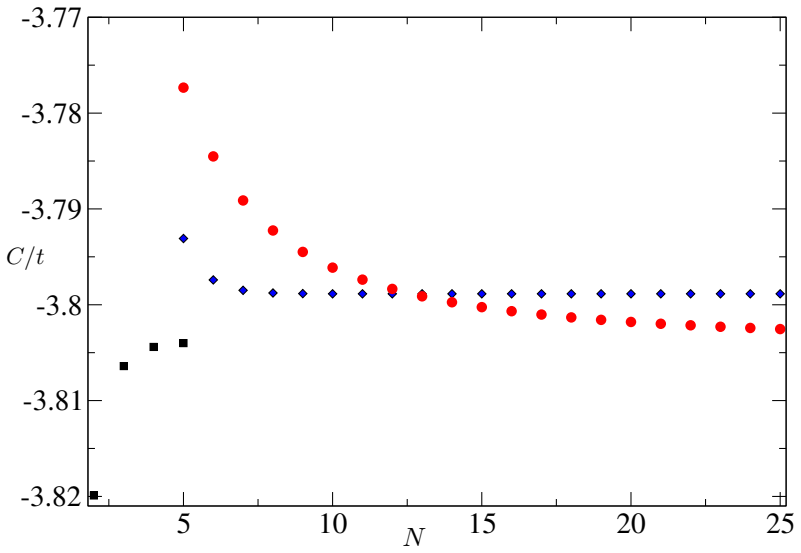

Figure 4.3: $C(N)$ calculated using different numerical techniques. The red dots represent DMRG results, the black squares are results from exact diagonalisation, and the blue diamonds are results obtained using a variational ansatz (see text). Note the scale for C/t. These results agree to a remarkable degree.

carry out some numerical investigations. We numerically diagonalise the system with periodic boundary conditions for $N \in [2, 5]$, and find that $C(N)$ converges toward a constant value very quickly: $C(5) - C(4) = \mathcal{O}(10^{-4}t)$. We also check the behaviour for larger systems, using DMRG results[2] provided by our collaborator, Gabriele de Chiara (note that Dr. de Chiara produced all of the DMRG data referenced in this chapter)[58, 59]. These results also show convergence towards a constant $C(N)$, although it is somewhat slower due to the open boundary conditions necessarily for a DMRG implementation. The energy in this case is converging around $N = 25$ (see Fig. 4.3). Thus, energetic considerations suggest that the ground state at one particle above critical filling contains two disrupted cells, while the rest of the crystal remains intact. We will use this insight to construct an ansatz for the low-lying eigenstates in the next section.

4.3.2 Low-energy ansatz

We now attempt to construct an ansatz for the low-energy behaviour of our system. Consider the ground state on a lattice with $L = 4N - 2$ sites. We suppose this to contain $N - 2$ localised flat band states. The remaining two particles must

[2]In this case we are forced to use open boundary conditions due to the DMRG implementation for the periodic sawtooth chain.

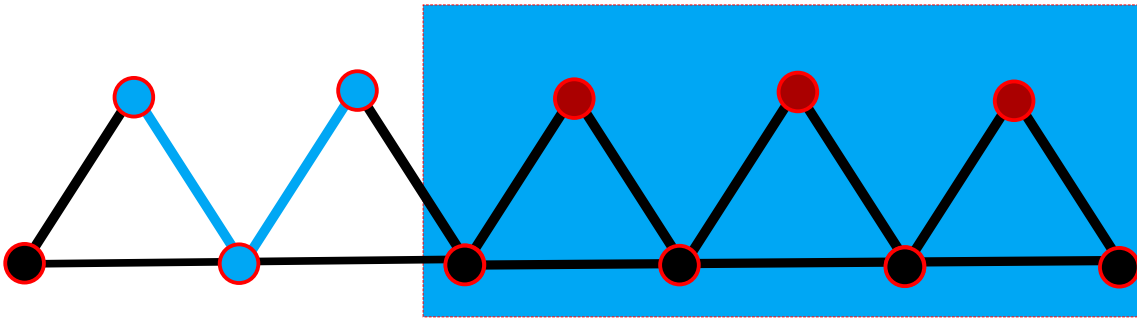

Figure 4.4: A component of the ansatz: the lattice is filled with localised eigenstates, except for a seven-site block, highlighted in blue here. The block contains two particles, which occupy the two-body ground state of the seven-site system. The ansatz is made of a superposition of such components, with the blue block starting on each lower site: the coefficients are used as variational parameters.

avoid overlapping with these states, and so are confined to a seven-site block (seven sites being the maximum size of a connected block within an otherwise-undisrupted crystal - see Fig. 4.4). We assume for simplicity that the wavefunction within the disrupted block is the ground state of the isolated seven-site system. This assumption is supported by the fact that the two-body ground state energy of the seven-site system, which may be calculated numerically, is close to $C(N)_{N\to\infty}$. Let $|\psi_i\rangle$ denote a state in which the disrupted block begins on the $2i$th site:

$$|\psi_i\rangle \equiv B_i^\dagger \prod_{l=1}^{N-2} V_{i+2l+2}^\dagger |0\rangle, \tag{4.13}$$

where $B_i^\dagger$ creates the two-body ground state over a seven-site block beginning on site $2i$. For later use, note that $B_i^\dagger$ has the form

$$B_i^\dagger = \sum_{j=0}^{5} \sum_{k=j+1}^{6} \alpha_{jk} b_{2i+j}^\dagger b_{2i+k}^\dagger, \tag{4.14}$$

with the α_{ij} complex numbers. Because $B_i^\dagger$ creates an eigenstate over the block, we have

$$HB_i^\dagger|0\rangle = E_B B_i^\dagger|0\rangle + X_i^\dagger|0\rangle, \tag{4.15}$$

where E_B is the seven-site ground state energy and $X_i^\dagger$ creates the terms that end up outside of the block upon the application of H:

$$X_i^\dagger = \sum_{j=0}^{5} \alpha_{j6} b_{2i+j}^\dagger (\sqrt{2} b_{2i+7}^\dagger + b_{2i+8}^\dagger) + \sum_{j=1}^{6} \alpha_{j0} b_{2i+j}^\dagger (\sqrt{2} b_{2i-1}^\dagger + b_{2i-2}^\dagger). \tag{4.16}$$

This will help to simplify future calculations. Finally, our ansatz is:

$$|\Psi\rangle = \sum_i \beta_i |\psi_i\rangle, \tag{4.17}$$

with the β_i complex numbers to be determined via the Ritz method.

4.3.3 Generalised eigenvalue problem and solution

We now obtain a generalised eigenvalue problem for our system (see Appendix A and Eq. (A.12). From Equations (4.13) and (4.15), we see that the action of H on $|\psi_i\rangle$ is

$$H|\psi_i\rangle = \prod_{l=1}^{N-2} V_{i+2l+2}^\dagger H B_i^\dagger|0\rangle - 2t(N-2)|\psi_i\rangle \tag{4.18}$$

$$= [E_B - 2t(N-2)]|\psi_i\rangle + \prod_{l=1}^{N-2} V_{i+2l+2}^\dagger X_i^\dagger|0\rangle \tag{4.19}$$

Using this in the equation for the β_i given by the Ritz method, which reads

$$\sum_j \langle\psi_i|H|\psi_j\rangle b_j = E\langle\psi_i|\psi_j\rangle b_j, \tag{4.20}$$

we obtain

$$\lambda \sum_j \langle \psi_i | \psi_j \rangle \beta_j = \sum_j \langle \psi_i | \prod_{l=1}^{N-2} V^\dagger_{j+2l+2} X^\dagger_j |0\rangle \beta_j, \tag{4.21}$$

where $\lambda = E - E_B + 2t(N-2)$. We solved the above using a routine [60] from the GNU scientific library. The solutions turn out to be rather interesting. Let us label them such that the jth component of the nth solution is $\beta_j^{(n)}$. Then, to machine accuracy, we find that the solutions to Eq. (4.21) are

$$\beta_j^{(n)} = (-1)^{jn} e^{ijk_n}, \tag{4.22}$$

$$\Rightarrow |\Psi^{(n)}\rangle = \sum_j (-1)^{jn} e^{ijk_n} |\psi_j\rangle, \tag{4.23}$$

where $k_n = 2\pi n/L$. We see that the disrupted block behaves like a single particle hopping on a lattice with $L/2$ sites (L being the number of sites in the original lattice). Its eigenstates are Bloch wave states, with quasimomenta k_n and Bloch functions $u^{(n)}(x) = (-1)^{xn}$. Of course, our method also reveals the dispersion relation for the block's motion, which is plotted in Fig. 4.5. It is quadratic at low momenta, with an effective mass of $m^*/t \approx 1.25$. This behaviour can be understood as a reflection of the dispersive nature of the upper band. Crudely, we can think of the extra particle as occupying the upper band and causing a defect in the crystal. The defect therefore inherits the upper band's dispersive behaviour, and propagates through the medium of flat band states with dispersion $E(k) = k^2/2.5t$.

4.3.4 Verification and proposed experimental signature

Our results were obtained using a variational principle which relies heavily on a good guess at the low-energy subspace. Results obtained with such an approach cannot be trusted *a priori* and must be verified. As a first step in this direction, we compare the value of $C(N)$ (see Eq. (4.12)) yielded by the variational calculation to the values obtained from exact diagonalisation and DMRG. In Fig. 4.3 the values of $C(N)$ from all three methods are plotted. We find excellent agreement between the variational result and the exact numerical calculations. For instance, once well-converged, the variational and DMRG results agree to within 0.1%. We can also access the low-lying

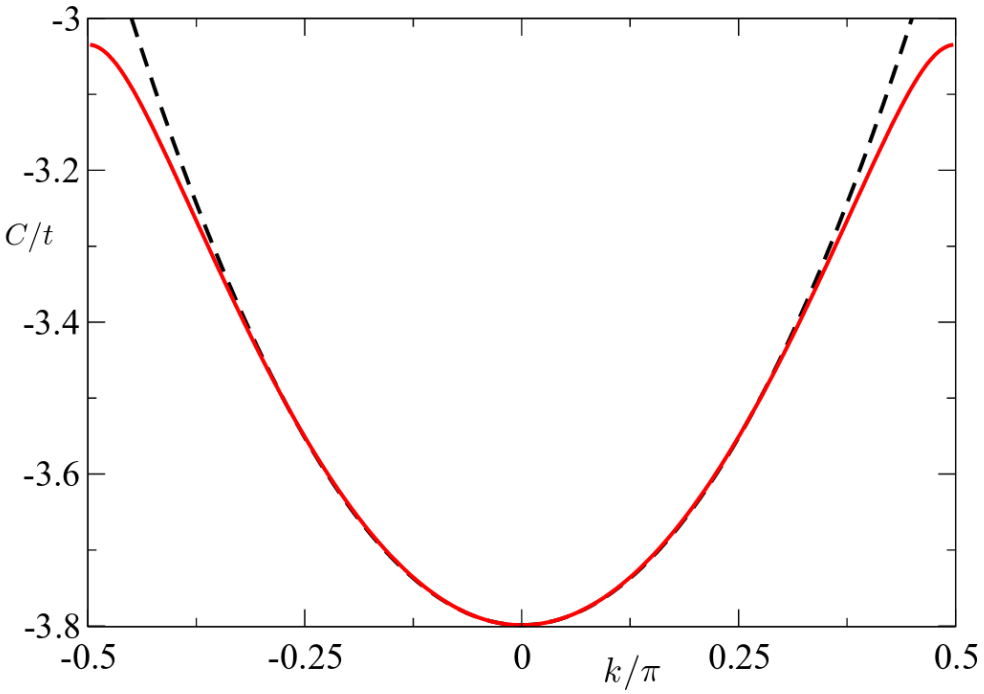

Figure 4.5: The dispersion relation for the disrupted block (solid red line) together with a quadratic function $f = k^2/2.5t$ (dashed black line). We see that the block's dispersion is quadratic at low energies, with effective mass $m^*/t = 1.25$.

excitations with exact diagonalisation (for small particle number), and we compare the energy of these with the corresponding variational energies. Fig. 4.6 shows the comparison. There is good agreement for the lowest five states, which is encouraging in such a small system. The results begin to diverge at higher energies, but this is to be expected: we only expect our ansatz to capture low-energy behaviour. The disagreement may be due to an excitation within the disrupted block, for instance, or the crystalline order may become disrupted outside of the seven sites.

Finally, we may probe the structure of the ground state by investigating its momentum distribution. This will further verify our ansatz, and, moreover, will provide an experimentally viable test of our theory [61, 62, 63]. Rather than considering the full momentum distribution, in which the contribution from the extra particle will be washed out by the localised states, we should calculate the change in momentum

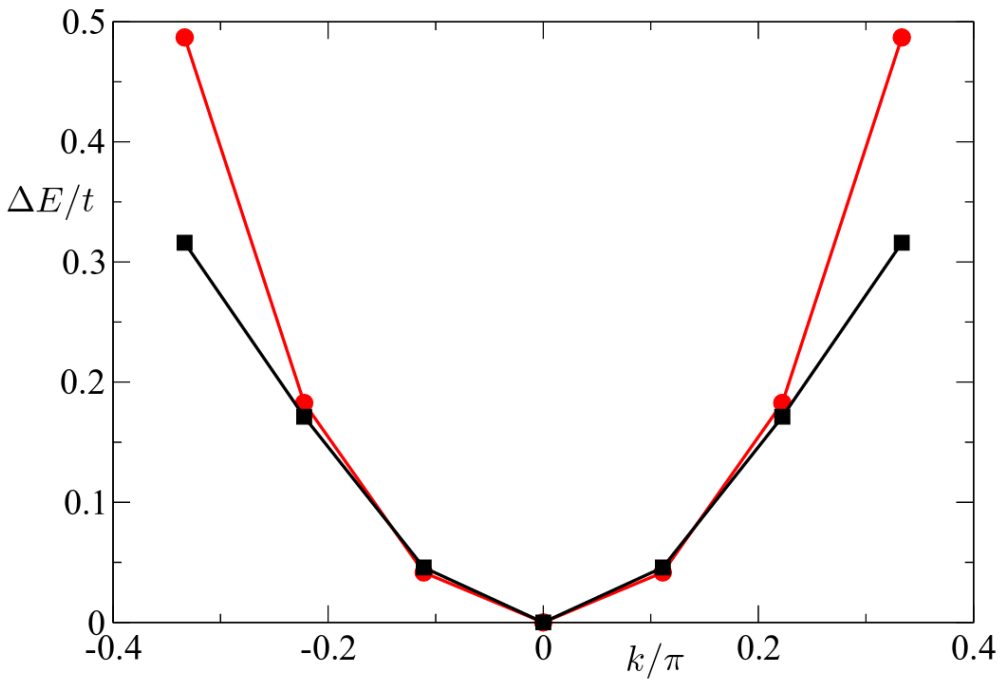

Figure 4.6: Comparison of variational (red circles) and exact (black squares) excitation energies of the seven lowest states, for a system of five particles.

distribution upon addition of the extra particle. For $N \leq N_c$ particles, we have

$$\langle \Psi^{(0)} | n_k | \Psi^{(0)} \rangle = \sum_{x,y} e^{i(x-y)k} \langle 0 | \left[\prod_i V_i \right] b_x^\dagger b_y \left[\prod_{i'} V_{i'}^\dagger \right] | 0 \rangle. \tag{4.24}$$

Using the fact that none of the localised states overlap when $\nu \leq \nu_c$, this is equal to

$$\begin{aligned} \sum_{x,y} e^{i(x-y)k} \langle 0 | \sum_{\beta=1}^{N} (\sqrt{2}\delta_{2\beta,x} - \delta_{2\beta+1,x} - \delta_{2\beta-1,x}) \left[\prod_{i \neq \beta} V_i \right] \\ \times \sum_{\alpha=1}^{N} \left[\prod_{i \neq \alpha} V_i^\dagger \right] (\sqrt{2}\delta_{2\alpha,y} - \delta_{2\alpha+1,y} - \delta_{2\alpha-1,y}) | 0 \rangle. \end{aligned} \tag{4.25}$$

Summing over the delta functions, we obtain

$$\langle \Psi^{(0)} | n_k | \Psi^{(0)} \rangle = N(\sqrt{2} - 2\cos(k))^2. \tag{4.26}$$

We can subtract this from the numerical results for $N = N_c + 1$, obtaining the right derivative $\partial_{n_k}/\partial_\nu|^+_{\nu=\nu_c}$, which clearly disagrees with the left derivative at this

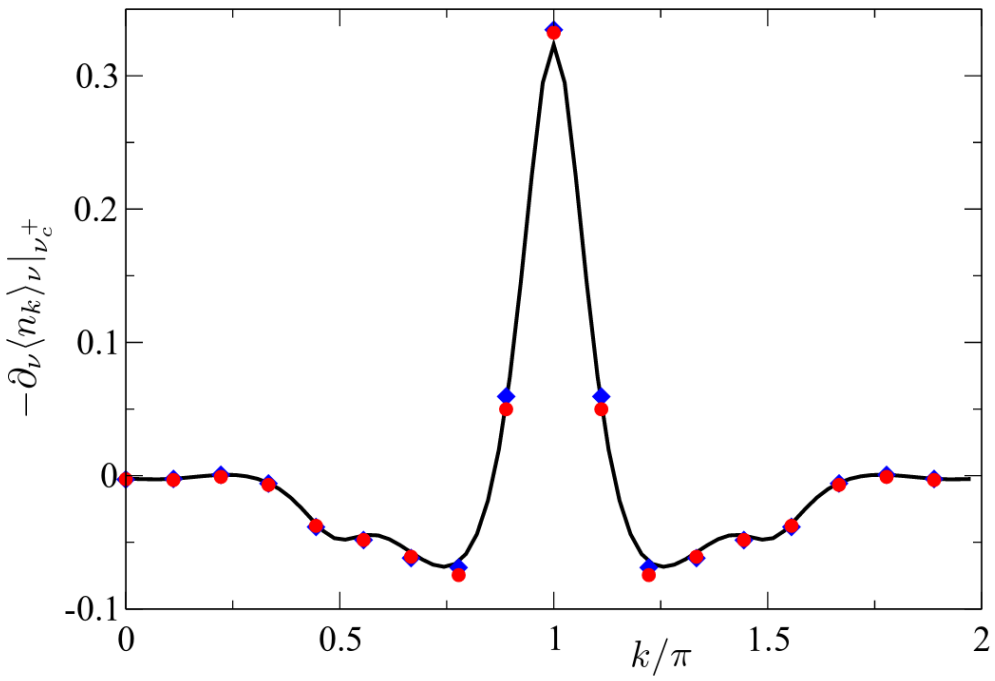

Figure 4.7: *Minus* the right derivative of momentum density as a function of filling fraction at critical filling, as obtained variationally with a twenty-particle system (black line), again variationally with a five-particle system (blue diamonds), and from exact diagonalisation with five particles (red circles).

point. The discontinuity in the momentum distribution indicates the disruption of the crystal phase. In Fig. 4.7 the right derivative obtained from our variational wavefunction is plotted, together with the derivatives from exact diagonalisation. We see that the variational and exact ground states have very similar momentum densities - note the close overlap for the five-particle calculations. Also, since our variational method is computationally inexpensive, we were able to calculate the derivative for a twenty-particle system for comparison with the five-particle data. We find a fine-grained oscillatory structure which agrees nicely with the exact five-particle points, with a strong peak that is also well-reproduced. This excellent agreement is definitive evidence that our ansatz is a good one, i.e., that the low-energy behaviour described here is the true low-energy behaviour of the system.

4.4 Summary and outlook

In this chapter we have explored the physics of a system whose lowest energy band is flat, and above the critical filling factor where the lattice is saturated with localised particles. We found that an extra particle added on top of the saturated system creates a defect, which can be regarded as a two-body bound state, confined to a seven-site block. The low-energy subspace of the system is spanned by states where this defect appears within an otherwise-intact crystal of localised particles. The low lying excitations see the defect moving through the medium with a quadratic dispersion. This dispersive behaviour has been inherited from the curved upper-band, which we argued must contribute to the low energy states above critical filling. It is worth commenting that the above description is transparent to a degree that is unusual in many-body physics: the behaviour of the system is easily understood in terms of its constituent bosons, and the structure of the low-lying many-body excitations is easily visualisable.

It would be interesting to explore the consequences of adding more than one particle on top of the saturated state. For instance, if the effect is to produce more defects, it may be possible to calculate their behaviour by modeling them as single particles and using scattering theory. Also, it is interesting to ask whether the kind of behaviour found here is a general feature of strongly interacting models with flat lowest energy bands.

Chapter 5

The fermionic Luttinger model

5.1 Introduction

The next two chapters are concerned with *Luttinger's model*, a very general and widely applicable model of one dimensional many-body quantum systems. Introduced by its namesake in 1963 [64], the model is actually a slightly modified version of the earlier *Tomonaga's model*, circa 1950 [1]. Tomonaga's interest at the time was in solving the interacting electron problem - Fermi liquid theory was still six years away - and he realised that this could be done after invoking a number of simplifying assumptions, which, unfortunately (from his point of view), included the assumption that electrons only move in one dimension. While Tomonaga's method failed to describe higher-dimensional electron systems, it laid the foundations for a remarkably powerful effective low-energy theory of the one-dimensional many-body problem. Tomonaga's insight was that 1D Fermi systems are best analysed in terms of their density wave excitations, which are approximately bosonic. He showed that the low-energy behaviour of the fermionic system, when described in terms of these bosonic excitations, has an approximate solution which becomes exact in the limit where the electronic density waves are exactly bosonic. Over a decade later, Luttinger [64], who was unaware of Tomonaga's work, published a closely related model. The fermionic density waves in Luttinger's model are exactly bosonic, and as a consequence it is exactly solvable. This exact solvability comes at a price, however; Luttinger's model appears rather esoteric compared with Tomonaga's, containing

as it does two species of fermion, each with its own dispersion and an infinitely deep, filled Fermi sea. One of the goals of the next chapter is to investigate the connection between Tomonaga's model, which has a completely clear relationship with the system it intends to describe, and Luttinger's model, which does not.

Although Luttinger's paper contains a solution to his model, it is incorrect; oddly enough, Luttinger failed to recognise the bosonic nature of the density waves. Two years after its publication, Mattis and Lieb [71], having rediscovered Tomonaga's work, corrected Luttinger's mistake and found the bosonic excitations, in terms of which they provided the model's exact solution. This development provided physicists with access to a large number of experimental predictions for a fairly broad class of one-dimensional systems; namely, those for which the approximations invoked in order to arrive at Tomonaga's model are valid. This class was significantly widened by Haldane [73], who gave arguments suggesting that most 1D systems behave at low energies as if they obey Tomonaga's model, even if they violate the approximations which lead to it - even, in fact, if they are not composed of fermions at all. Haldane termed this new universality class the *Luttinger liquid*, and introduced a general method for modeling its members, which is nowadays referred to as *field theoretic bosonisaton* (as opposed to the more traditional *constructive* bosonisation, à la Tomonaga and Luttinger). The universality hypothesis (or *Luttinger liquid hypothesis*) has since been successfully tested using exactly-solvable examples [74], and has received strong theoretical support from renormalisation group methods and numerical simulations [75, 76, 77] .

Experimentally, signatures of Luttinger liquid behaviour have been observed in a wide variety of effectively one-dimensional systems including carbon nanotubes [78, 79, 80, 81], nanowires [82, 83, 84], and optical lattices [61, 85].

In preparation for the next chapter, which is a detailed exploration of the relationship between Luttinger's model and the underlying microscopic physics, we give here a basic description of the model and its solution via bosonisaion.

5.2 Constructive bosonisation

Bosonisation is the most widely-employed technique for investigating Luttinger liquid behaviour. There are two flavours of bosonisation: *field-theoretic*, as introduced by Haldane [73], and *constructive*, which is based on the earlier work of Tomonaga [1]. In the constructive approach, one begins with a microscopic Hamiltonian, makes a number of approximations, and ends up with an exactly solvable model (referred to as Luttinger's model). The field-theoretic formalism, on the other hand, is a manifestation of the Luttinger liquid hypothesis mentioned above, and was invented as a means of applying bosonisation in cases where the approximations necessary for constructive bosonisation are not straightlforwardly valid, and to systems that are already bosonic. It is a phenomenological approach which assumes Luttinger liquid behaviour from the outset, and yields relations between experimental quantities. Thus, with field-theoretic bosonisation one gains in generality, but loses in clarity and connection with the microscopic physics. Since the goal of the next chapter will be to describe the relation between Luttinger's model and the microscopic physics from which it emerges, and to highlight a misconception found in the literature on the constructive approach, we will ignore field-theoretic bosonisation and work exclusively with the constructive formalism, of which this section gives a sketch.

5.2.1 Fermionic model

Bosonisation was originally applied to systems of one-dimensional spin-polarised fermions, and we will give our account in that context. Thus, consider the following microscopic Hamiltonian:

$$H = \frac{\hbar^2}{2m} \sum_k k^2 c_k^\dagger c_k + \hat{V}, \tag{5.1}$$

where

$$\hat{V} = \frac{1}{2L} \sum_{kk'q} V(q) c_{k+q}^\dagger c_{k'-q}^\dagger c_{k'} c_k, \tag{5.2}$$

and

$$V(q) = \int_{-\infty}^{\infty} dx\, e^{iqx} W(x), \tag{5.3}$$

with $W(x)$ a realistic two-body interaction. Here c_k is a fermionic momentum space annihilation operator satisfying $\{c_k, c_{k'}^\dagger\} = \delta_{k,k'}$.

To reduce the above to an exactly solvable model, one must replace the realistic interaction with a much simpler one. To this end, note that, provided $V(q)$ is not too strong, the above model's low-energy sector will not include states containing highly excited particles: it will consist entirely of Fermi-sea-like states with excitations about the Fermi points. This observation is useful, because the interaction can only lead to a few different processes if one restricts to states of this type. For $|q| \ll k_F$, two particles on the same branch may exchange momentum, which we will refer to as an *intrabranch* process, or two particles on opposite branches may exchange momentum, which we will call an *interbranch* process. For $|q| \approx 2k_F$, two particles may swap branches, also an interbranch process. These processes are shown in Fig. 5.1; all others are forbidden at low energies, since they result in a large increase in kinetic energy. If particles are confined to a narrow enough range of momenta about the Fermi points, it is reasonable to approximate the potential $V(q)$ as a constant for each of these processes. When the particles swap branches, one may set $V(q) = V(2k_F)$; otherwise, $V(q) = V(0)$. Under this approximation, restricting to a space containing no particles higher than $\pm(k_F + \Lambda)$ and no holes deeper than $\pm(k_F - \Lambda)$, and including only the interactions enumerated above, the interaction becomes

$$V = \frac{1}{2L}\left(\sum_{k,k',q\in I_2} g_2^{(0)} + \sum_{k,k',q\in I_4} g_4^{(0)}\right) c_{k+q}^\dagger c_{k'-q}^\dagger c_{k'} c_k, \tag{5.4}$$

where $g_2^{(0)} = V(0) - V(2k_F)$ (this form is due to fermionic statistics, as we will see), $g_4^{(0)} = V(0)$, and I_2 restricts the sum to interbranch scattering, and I_4 to intrabranch - the sets are cumbersome to write explicitly, but it should be clear what values they contain.

The other approximation one must invoke in order to arrive at an exactly-solvable model involves linearising the dispersion relation. It is clear that this is a sensible

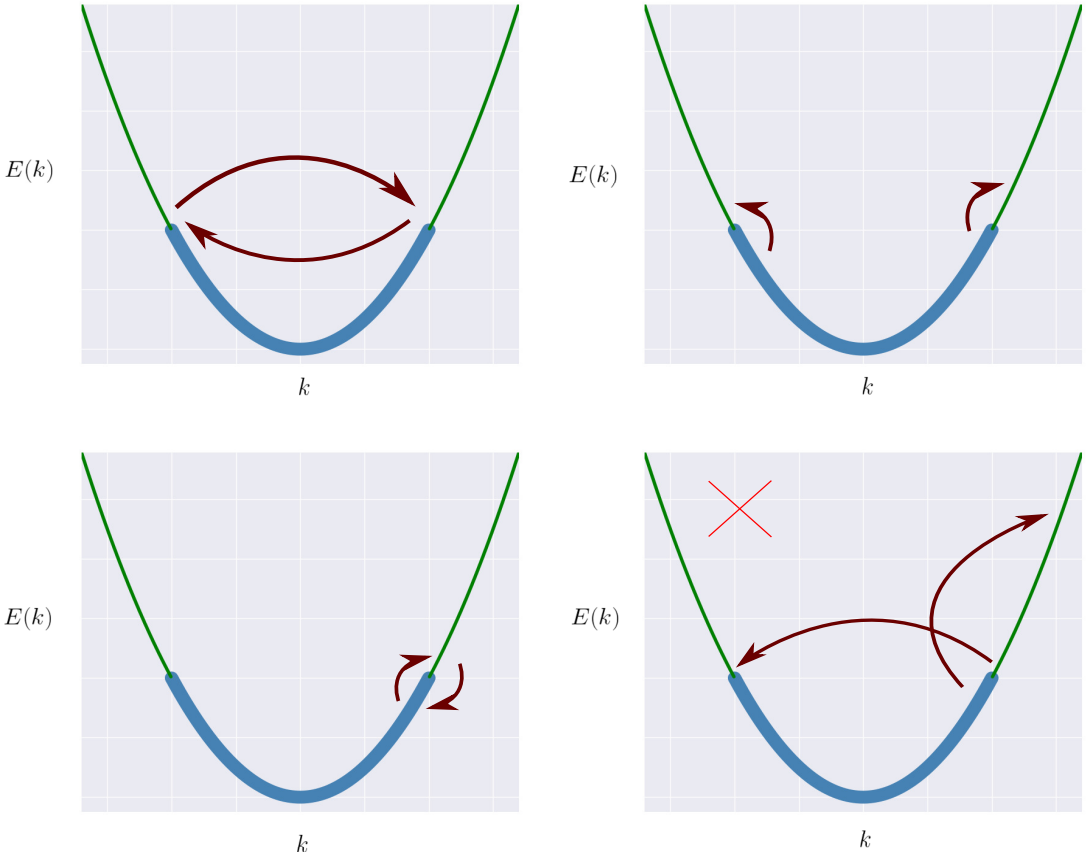

Figure 5.1: The various types of process produced by the interaction (see text). The blue section of the dispersion represents the filled Fermi sea, and the green part the unoccupied states. Note that the bottom right process, and other processes of this kind, will not occur at low energies, since they cause too large an increase in kinetic energy.

procedure at low energies, since $(k_F + \delta k)^2 \approx k_F^2 + 2k_F\delta k$. Upon carrying it out, the model's parameters become renormalised: $g_{2,4}^{(0)} \to g_{2,4}$, where g_2 is supposed to reproduce the realistic interbranch scattering properties, and g_4 the intrabranch. We will have much more to say about this in the next chapter.

The final step towards Luttinger's model is rather unusual: one switches to a different, seemingly very contrived model. The low energy physics of this new model matches that of the old, but it has the advantage of being exactly solvable by bosonisation, as we will soon see. The new model contains two species of particles, *left movers* and *right movers*, each with unbounded momenta $k \in (-\infty, \infty)$. The right movers have dispersion $\epsilon(k) = v_F k$, and for the left movers, $\epsilon(k) = -v_F k$, where v_F is the Fermi velocity of the original model. The branches are coupled by

the interaction

$$V_{\text{inter}} = \frac{1}{2L} \sum_{k>0,k'<0,q\neq 0} g_2 \, c^\dagger_{R,k} c_{R,k+q} c^\dagger_{L,k'} c_{L,k'-q} + (R \leftrightarrow L), \tag{5.5}$$

where $c^\dagger_{R,k}$ creates a right mover of momentum k, and $\{c_{\eta,k}, c_{\eta',k'}\} = \{c^\dagger_{\eta,k}, c^\dagger_{\eta',k'}\} = 0$, $\{c_{\eta,k}, c^\dagger_{\eta,k'}\} = \delta_{\eta,\eta'}\delta_{k,k'}$. There is also an intrabranch interaction,

$$V_{\text{intra}} = \frac{1}{2L} \sum_{k>0,k'<0,q\neq 0} g_4 \, c^\dagger_{R,k} c_{R,k+q} c^\dagger_{R,k'} c_{R,k'-q} + (R \leftrightarrow L). \tag{5.6}$$

This is Luttinger's model. Although it seems odd, if one fills the infinite "Fermi sea" of each branch, it is not difficult to imagine how it might agree with the original model at low energies.

5.2.2 Bosonisation

5.2.2.1 Momentum space operators

We now show that the two-branch model introduced above admits a simple bosonic representation. Consider the operator

$$\rho_{\eta,k} = \sum_q c^\dagger_{\eta,k+q} c_{\eta,q}, \tag{5.7}$$

where $k > 0$. We will show that this operator, under a very simple modification, obeys bosonic commutation relations. These commutation relations can be exploited to write the Luttinger's model in a form that can be solved via a Bogoliubov transformation.

In order to avoid unnecessary mathematical difficulties, we restrict to a space where all states have a lowest hole, below which every state is occupied, and a highest particle, above which all states are unoccupied. Let the momentum of the lowest hole be k_-, and that of the highest particle be k_+. The commutator's restriction to this space is all that is needed, since a real Luttinger liquid will contain neither an infinitely excited particle, nor an infinitely deep hole. The action of the $\rho_{\eta,k}$ upon vectors in this restricted space can generate only a finite number of terms;

since the result of an infinite sum of vectors depends on the order of the terms, this restriction gives us the freedom to rearrange the sums. Care must still be taken, however, as infinite series can appear in the calculation even if the total sum is finite. In particular, consider the product

$$\rho_{\eta,k}\rho_{\eta',k'} = \sum_{q,q'} c^\dagger_{\eta,q+k}c_{\eta,q}c^\dagger_{\eta',q'+k'}c_{\eta',q'} \tag{5.8}$$

$$= \delta_{\eta,\eta'}\sum_{q} c^\dagger_{\eta,q+k}c_{\eta,q-k'} - \sum_{q,q'} c^\dagger_{\eta,q+k}c^\dagger_{\eta',q'+k'}c_{\eta,q}c_{\eta',q'}. \tag{5.9}$$

Both sums in Eq. (5.9) are finite in our restricted space, except when $k' = -k$. In that case, because of the filled Fermi sea, the first term will give infinity. Therefore we will have to treat the case $k' = -k$ carefully. Concentrating on the case when $k' \neq -k$ for now, then, one obtains

$$[\rho_{\eta,k}, \rho_{\eta',k'}] = \delta_{\eta,\eta'}\sum_{q=-\infty}^{\infty}(c^\dagger_{\eta,q+k}c_{\eta,q-k'} - c^\dagger_{\eta,q+k+k'}c_{\eta,q}) \tag{5.10}$$

$$= \delta_{\eta,\eta}\sum_{q=k_--k}^{k_++k'} c^\dagger_{\eta,q+k}c_{\eta,q-k'} - \delta_{\eta,\eta}\sum_{q=k_--k'-k}^{k_+} c^\dagger_{\eta,q+k+k'}c_{\eta,q}. \tag{5.11}$$

Shifting $q \to q + k'$ in the first sum, one finds that $[\rho_{-k}, \rho_{k'}] = 0$. For the $k' = -k$ case, it is convenient to work with the product (5.8) rather than directly with the commutator. Anticommuting the η operators past the η' gives

$$\rho_{\eta,k}\rho_{\eta',-k} = \delta_{\eta,\eta'}\left(\sum_{q=k_-+k}^{k_+} c^\dagger_{\eta,k}c_{\eta,k} - \sum_{q=k_-+k}^{k_+} c^\dagger_{\eta,q-k}c_{\eta,q-k} + \sum_{\substack{q=k_++k\\ q'=k_--k}}^{k_+} c^\dagger_{\eta,q-k}c_{\eta,q}c^\dagger_{\eta,q'-k}c_{\eta,q'}\right). \tag{5.12}$$

Sending $k \to -k$ in the above expression and subtracting yields the commutator:

$$[\rho_{\eta',-k}, \rho_{\eta,k}] = \delta_{\eta,\eta'}\sum_{q=k_--k}^{k_-} c^\dagger_{\eta,q}c_{\eta,q}. \tag{5.13}$$

Since all levels below k_- are occupied, we finally have

$$[\rho_{\eta',-k}, \rho_{\eta,k}] = \delta_{\eta,\eta'} \frac{Lk}{2\pi}. \tag{5.14}$$

Clearly, then, the operator

$$a_{\eta,k} = i\sqrt{\frac{2\pi}{Lk}} \rho_{\eta,k} \tag{5.15}$$

is *bosonic*, that is to say,

$$[a_{\eta,k}, a^\dagger_{\eta',k'}] = \delta_{\eta,\eta'} \delta_{k,k'}. \tag{5.16}$$

5.2.2.2 Position space operators

It is also useful to obtain a position-space representation of the relationship between bosonic and fermionic degrees of freedom. Following [65], we do so using the fact that $\psi_\eta(x)|F\rangle$ is an eigenstate of $a_{\eta,k}$, where $|F\rangle$ is the Fermi sea (the state with both branches full up to their Fermi points) and $\psi_\eta(x)$ annihilates an η-mover at x. As such, $\psi_\eta(x)|F\rangle$ admits a coherent state representation in terms of the $a^\dagger_{\eta,k}$. To see this, compute the commutator

$$[a_{\eta,k}, \psi_{\eta'}(x)] = -\sum_{q,q'} \frac{2\pi}{L\sqrt{k}} [c^\dagger_{\eta,q-k} c_{\eta,k}, e^{ik'x} c_{\eta,k'}], \tag{5.17}$$

which can be evaluated by noting that

$$\begin{aligned}
c^\dagger_{\eta,q-k} c_{\eta,k} c_{\eta',k'} &= -c^\dagger_{\eta,k-q} c_{\eta',k'} c_{\eta,k} && (5.18)\\
&= c_{\eta',k'} c^\dagger_{\eta,k-q} c_{\eta,k} - \{c^\dagger_{\eta,k-q}, c_{\eta,k'}\} c_{\eta,k} && (5.19)\\
&\Rightarrow [c^\dagger_{\eta,k-q} c_{\eta,k}, c_{\eta',k'}] = -\delta_{\eta,\eta'} \delta_{k-q,k'} && (5.20)\\
&\Rightarrow [a_{\eta,k}, \psi_{\eta'}(x)] = i\delta_{\eta,\eta'} \sqrt{\frac{2\pi}{Lk}} e^{ikx} \psi_{\eta'}(x). && (5.21)
\end{aligned}$$

Also, it is easy to see that $a_{\eta,k}$ annihilates $|F\rangle$. Therefore,

$$a_{\eta',k} \psi_\eta(x)|F\rangle = i\delta_{\eta,\eta'} \sqrt{\frac{2\pi}{Lk}} \psi_\eta(x)|F\rangle, \tag{5.22}$$

as claimed. Before giving the coherent state representation in terms of bosnic creation operators, we must introduce new operators K_η, called *Klein factors*. The Klein factors are defined through their action on $|F\rangle$,

$$K_\eta|F\rangle = c_{\eta,k_F}|F\rangle. \tag{5.23}$$

In other words, they remove the topmost particle from the η-moving Fermi sea. They are necessary because $\psi_\eta(x)$ annihilates a fermion, while the $a_{\eta,k}$ conserve fermion number; thus, in order to relate the two, we need to augment $a_{\eta,k}$ by combining it with a fermion annihilation operator. Annihilating the topmost particle from the Fermi sea gives another Fermi sea, which is also annihilated by the $a_{\eta,k}$, and upon which a coherent state representation in terms of the $a^\dagger_{\eta,k}$ may therefore be built [67]. This representation is

$$\psi_\eta(x)|F\rangle = \exp\left(\sum_k \sqrt{\frac{2\pi}{Lk}} e^{ikx} a^\dagger_{\eta,k} - i\delta\right) K_\eta|F\rangle \tag{5.24}$$

$$\equiv e^{-i(\phi^\dagger_\eta(x)+\delta)} K_\eta|F\rangle \tag{5.25}$$

where $\delta \to 0$ in the $L \to \infty$ limit (we ignore it in the following). Having found the bosonic form for $\psi_\eta(x)$ acting on the Fermi sea, it is easy to generalise to the whole Hilbert space. This is because the $a^\dagger_{\eta,k}$ span every constant-particle-number subspace of the Fermionic model (this is proven in [65]), meaning that an arbitrary state with fixed fermion number can be written as $|\psi\rangle = f(\{a^\dagger_{\eta,k}\})|F\rangle$, where $f(\{a^\dagger_{\eta,k}\})$ is some function of the $a^\dagger_{\eta,k}$. One finds

$$\psi_\eta(x) = \lim_{\alpha\to\infty} \sqrt{\alpha} K_\eta e^{-i\varphi_\eta(x)}, \tag{5.26}$$

where $\varphi(x) = \phi^\dagger(x) + \phi(x)$ and the $\alpha \to \infty$ limit will be explained in the next chapter.

5.2.2.3 The Hamiltonian

We are now in a position to bosonise the fermionic Luttinger model, beginning with the interaction (5.5), which can be bosonised by direct inspection. We have

$$V_{\text{inter}} = \frac{g_2}{2L} \sum_{q=-\infty}^{\infty} \rho_{R,-q}\rho_{L,q} + (R \leftrightarrow L) \tag{5.27}$$

$$= \frac{g_2}{2\pi} \sum_{q>0} q \left[a^\dagger_{L,q} a^\dagger_{R,q} + a_{L,q} a_{R,q} \right]. \tag{5.28}$$

Similarly, for the intrabranch term,

$$V_{\text{intra}} = \frac{g_4}{2\pi} \sum_{q>0} q \left[a^\dagger_{R,q} a_{R,q} + a^\dagger_{L,q} a_{L,q} \right]. \tag{5.29}$$

As for the kinetic term, by standard manipulations one can show that

$$[H_{\text{kin}}, a^\dagger_{\eta,k}] = v_F k a^\dagger_{\eta,k}. \tag{5.30}$$

This, together with the canonical commutation relations (5.16), implies that

$$H_{\text{kin}} a^\dagger_{\eta,k} |F\rangle = (v_F k + E) a^\dagger_{\eta,k} |F\rangle, \tag{5.31}$$

with E the kinetic energy of $|F\rangle$. We see that the $a^\dagger_{\eta,k}$ create eigenstates of H_{kin} on top of the Fermi sea, which acts as a kind of vacuum state. Therefore, H_{kin} must admit a diagonal representation in the basis created by the $a^\dagger_{\eta,k}$ acting on $|F\rangle$, and so we have

$$H_{\text{kin}} = v_F \sum_{q>0} q \left[a^\dagger_{L,q} a_{L,q} + a^\dagger_{R,q} a_{R,q} \right], \tag{5.32}$$

where we have neglected a chemical potential.

5.2.3 Solving the model

The bosonic form of Luttinger's model derived in the previous section can be solved by a Bogoliubov transformation, as we now demonstrate. To begin with, it is convenient to combine the contributions from the intrabranch and kinetic terms by

defining a modified Fermi velocity, $v = v_F + g_4/2\pi$. Then the Hamiltonian can be written in matrix form as

$$H = V^\dagger M V, \tag{5.33}$$

where

$$M = \begin{pmatrix} vq & qg_2/2\pi & 0 & 0 \\ qg_2/2\pi & vq & 0 & 0 \\ 0 & 0 & vq & qg_2/2\pi \\ 0 & 0 & qg_2/2\pi & vq \end{pmatrix}, \tag{5.34}$$

and

$$V = \begin{pmatrix} a_{L,q} \\ a^\dagger_{R,q} \\ a_{R,q} \\ a^\dagger_{L,q} \end{pmatrix}, \tag{5.35}$$

and we have once again thrown away an irrelevant constant term. If the above matrix can be made diagonal in a basis of new operators which obey canonical commutation relations, the Hamiltonian itself will be diagonal in the basis created by those new operators acting on $|F\rangle$. Let us assume that this is possible, and denote a new operator by $b^\dagger_{L,q}$, for example. It is clear from the structure of the matrix that we need only solve

$$S^\dagger \tilde{M} S = \mathrm{Diag}(\alpha_1, \alpha_2), \tag{5.36}$$

where

$$\tilde{M} = \begin{pmatrix} vq & qg_2/2\pi \\ qg_2/2\pi & vq \end{pmatrix}, \tag{5.37}$$

and

$$S \begin{pmatrix} b_{L,q} \\ b^\dagger_{R,q} \end{pmatrix} = \begin{pmatrix} a_{L,q} \\ a^\dagger_{R,q} \end{pmatrix}. \tag{5.38}$$

In order to preserve canonical commutation relations, we must set $s_{11} - s_{12} = 1$, $s_{11} = s_{22}$, and $s_{12} = s_{21}$, where the s_{ij} are the elements of S. Thus,

$$S = \begin{pmatrix} \cosh\theta & \sinh\theta \\ \sinh\theta & \cosh\theta \end{pmatrix}, \tag{5.39}$$

with θ some real parameter, which we solve for by plugging the above into Eq. (5.36). We obtain

$$K = e^{2\theta} = \sqrt{\frac{1 - g_2/2\pi v}{1 + g_2/2\pi v}}, \tag{5.40}$$

$$\alpha_1 = \alpha_2 = 2vq, \tag{5.41}$$

where K is the so-called Luttinger parameter. Given K, then, one has a diagonal representation of the Hamiltonian, and thus easy access to many aspects of the system's behaviour. In other words, if the approximations invoked to pass from the microscopic model to Luttinger's are valid, all one needs to do in order to obtain a complete description of the system's low-energy dynamics is calculate g_4 and v. This is clearly a very powerful technique, and the fact that it is possible shows that there is a great deal of universality in the low-energy behaviour of one-dimensional Fermi systems.

5.2.4 Example: correlation functions

Linear response theory provides, via Kubo formulae, relations between correlation functions and experimentally measurable quantities: if one knows all correlation functions for a particular system, one can easily calculate the system's response to any external perturbation, as long as the perturbation is weak enough so that the response is linear. One of the advantages conferred by bosonisation is the ability to easily calculate correlation functions. Since our interest in the next chapter is towards the microscopic interpretation of Luttinger's model rather than its macroscopic consequences, we will do no more than demonstrate this with a quick sketch of the calculation for a single-particle correlation function at zero temperature.

To begin with, let us write down the relationship between a microscopic position-space annihilation operator and its counterparts in Luttinger's model:

$$\psi(x) = \lim_{\alpha\to\infty} \frac{1}{\sqrt{\alpha}} \left(e^{-ik_F\alpha x}\psi_L(x) + e^{ik_F\alpha x}\psi_R(x)\right). \tag{5.42}$$

We will prove this relation in the next chapter. It is useful to calculate the equal-time one-particle correlation function in the non-interacting ground state first. This is

$$\langle\psi^\dagger(x)\psi(0)\rangle \propto e^{-ik_F\alpha x}\langle\psi_R^\dagger(x)\psi_R(0)\rangle + e^{ik_F\alpha x}\langle\psi_L^\dagger(x)\psi_L(0)\rangle. \tag{5.43}$$

Using the bosonisation formula (5.26) and the fact that the Klein factors commute with the boson fields, we have

$$\begin{aligned}
\langle\psi_\eta^\dagger(x)\psi_\eta(0)\rangle &\propto \langle e^{i\varphi_\eta(x)}e^{-i\varphi_\eta(0)}\rangle, &(5.44)\\
&= e^{[\varphi_\eta(x),\varphi_\eta(0)]/2}\langle e^{i(\varphi_\eta(x)-\varphi_\eta(0))}\rangle, &(5.45)\\
&= -\mathrm{sgn}(x)\langle e^{i(\varphi_\eta(x)-\varphi_\eta(0))}\rangle, &(5.46)
\end{aligned}$$

where the second line is obtained via the Baker-Campbell-Hausdorff formula, and the last uses the fact that $[\varphi_\eta(x), \varphi_\eta(0)] = -\mathrm{sgn}(x)$ [65]. In order to evaluate the expectation value, one may use the cumulant theorem $\langle\exp\left(f(b,b^\dagger)\right)\rangle = \exp\left(\langle f^2(b,b^\dagger)\rangle\right)$, with $f(b,b^\dagger)$ any quadratic in bosonic creation and annihilation operators [66]. This, together with the fact that the non-interacting ground state is the vacuum for bosons, so that $a_k|F\rangle = 0\ \forall k$, yields

$$\langle\psi_\eta^\dagger(x)\psi_\eta(0)\rangle \propto \exp\sum_{n>0}\frac{-1}{n}\left(e^{i\frac{2\pi n}{L}x}-1\right)\left(e^{-i\frac{2\pi n}{L}x}-1\right). \tag{5.47}$$

Finally, using the series $\sum_{n>0} e^{an}/n = -\ln(1-e^a)$ in the above equation, plugging the resulting expression for $\langle\psi_\eta^\dagger(x)\psi_\eta(0)\rangle$ into Eq. (5.43), and taking the limit $L\to\infty$, one finds

$$\langle\psi^\dagger(x)\psi(0)\rangle = \frac{\sin(k_F x)}{\sqrt{\alpha}\sin(\frac{\pi}{L}x)}, \tag{5.48}$$

The exact solution of Luttinger's model found in the previous section makes gen-

eralising to the interacting case rather simple. In terms of Bogoliubov-transformed operators, one finds

$$\langle \psi_R^\dagger(x)\psi_R(y)\rangle \propto e^{[\varphi_\eta(x),\varphi_\eta(y)]/2}\langle e^{i(\tilde{\varphi}_R(x)-\tilde{\varphi}_R(y))\cosh(\theta)}\rangle\langle e^{i(\tilde{\varphi}_L(x)-\tilde{\varphi}_L(y))\sinh(\theta)}\rangle, \tag{5.49}$$

where the expectation value is over the interacting ground state, and we have used the cumulant theorem again. Here $\tilde{\varphi}_\eta(x)$ has precisely the same expansion in terms of the Bogoliubov-transformed operators $b_{\eta,k}$ as does $\varphi_\eta(x)$ in terms of the original operators $a_{\eta,k}$, so that we can immediately write down the result

$$\langle \psi^\dagger(x)\psi(0)\rangle = \frac{\sin(k_F x)}{|\sqrt{\alpha}\sin(\frac{\pi}{L}x)|^{(K+1/K)/2}}, \tag{5.50}$$

where the last equality follows from the definition of K in terms of θ. This power-law decay of correlation functions is a general characteristic of Luttinger liquid behaviour.

Chapter 6

The microscopic origin of phenomenological parameters in Luttinger's model

6.1 Introduction

Luttinger's model is highly phenomenological. It contains three non-universal parameters: g_2, g_4, and v_F. In the previous chapter, we gave an interpretation of these parameters that is often encountered in the literature on constructive bosonisation, according to which g_2 and g_4 are related to interbranch and intrabranch scattering processes, respectively [86, 87, 88, 66]. In general these scattering processes are fantastically complicated, involving intractable many-body processes (*many* meaning greater than three here), so that renormalising the parameters in favour of realistic scattering data is impossible in practice. This is not a problem from an empirical point of view: it takes only one measurement to determine the Luttinger parameter, after which one can predict many other quantities of interest for the experimental system at hand; a procedure that is no more objectionable than fixing the charge on an electron or the gravitational constant by observation[1]. The Luttinger parameter is also calculable via heavy-duty numerical techniques such as DMRG [89, 90] and

[1]This claim is made from the point of view that these "fundamental" constants are not actually fundamental, but emerge from underlying, as yet unknown physics (which may not be true, of course).

Monte Carlo [91, 92], and via a recently-introduced method relying on few-body scattering (which exploits the ideas presented in this chapter) [93]. Proceeding in this manner, however, does not allow for any verification of the parameters' microscopic interpretation, which, from a less pragmatic standpoint, seems unsatisfactory. If we are to claim a degree of understanding, we should care whether that understanding is correct or not. Incorrect assumptions may cause practical problems too. For instance, one might be led to ask misleading or irrelevant questions.

The main aim of this chapter is to test the usual interpretation of g_2 and g_4. To see how this is possible, note that the relationship between underlying microscopic physics and macroscopic theory is well understood in several cases, sometimes to the extent that the effective theory's parameters are easily calculable from two-body physics - as we have seen, the theory describing Bose-Einstein condensation in the dilute limit is a prominent example. Taking inspiration from this, we construct Luttinger's model as an effective theory for a system that is simple enough to allow one to keep track of the relevant microscopic quantities. We consider a dilute 1D system of spin-polarised fermions, so that two-body scattering is the dominant interaction process, and construct an effective theory from the bottom up, replacing the full Hamiltonain by a simpler one (in this case Luttinger's Hamiltonian) that reproduces the pertinent realistic microscopic properties at the relevant energy. If the usual interpretation of g_2 and g_4 is correct, g_2 will appear as a parameter to be tuned to give the realistic two-body phase shift for interbranch scattering, and g_4 the same for intrabrach processes. We find, however, that tuning g_4 to reproduce intrabranch scattering properties is impossible. This is because two-body intrabranch scattering in Luttinger's model is pathological. Also, the intrabranch phase shift for spin-polarised 1D fermions vanishes at the relevant energy, making it an irrelevant microscopic process. On the other hand, conservation of charge requires a finite g_4 [86]. We conclude that g_4 is unrelated to intrabranch scattering; instead, we find that its role is to account for the energy shift exerted upon density wave excitations by the interbranch interaction. By showing that the usual interpretation of g_4 fails for this simple realisation of Luttinger's model, we cast serious doubt on its validity

in general.

While constructing Luttinger's model as an effective theory, we uncover its relationship with Tomonaga's. The extent to which density waves in Tomonaga's model fail to be bosonic turns out to be inversely proportional to the Fermi energy, leading us to take the Fermi points to infinity (the infinite-density limit). We are able to do this in such a way that the resulting dispersion relation is exactly linear, interbranch scattering properties are preserved, and the unbounded-from-below Hilbert space of Luttinger's model is obtained.

6.1.1 Renormalisation and Tomonaga

In this chapter we will construct an effective theory of 1D Fermi systems at low energies. It is crucial that our effective model correctly reproduces the aspects of the microscopic physics from which the universal low-energy behaviour emerges. Hence, we need to understand what it means for two models to produce the same physics. In particular, it is very important to realise that two Hamiltonians which agree approximately within a certain energy window will not necessarily produce similar physics, even at energies where they agree. For instance, consider the T-matrix from scattering theory, which satisfies

$$\langle k|T(z)|k'\rangle = \langle k|V|k'\rangle + \int dq\, \frac{\langle k|V|q\rangle\langle q|T(z)|k'\rangle}{z - E_q}. \tag{6.1}$$

It is clear that the T-matrix, and hence the scattering wavefunction, depends on the whole potential. So, two potentials that are approximately the same for a range of momenta may still produce markedly different scattering states within that range, if they disagree elsewhere. If we want a simplified potential to approximate the scattering given by a more complicated interaction, we have to adjust, or renormalise, its parameters. This idea will play an important role in our treatment.

Renormalisation was invented in the context of quantum electrodynamics. There, scattering amplitudes are divergent, but these divergences can be removed by adjusting the interaction parameters to absorb the infinities. The procedure was hugely controversial when it was first introduced, but, thanks largely to Wilson, it has

since been clarified, and to quite a remarkable extent. We now understand that quantum electrodynamics - and indeed the standard model - is an effective theory, which captures the essential low-energy behaviour of some deeper, unknown, underlying theory. It so happens that the interactions appearing in this effective theory lead to divergent scattering amplitudes, but this does not matter: the interaction parameters must be adjusted so that the effective theory reproduces the scattering properties of the deeper theory, as measured by experiment, and this adjustment removes the infinities.

Interestingly, Tomonaga, one of the originators of the renormalisation idea, failed to take account of precisely these ideas when working on his bosonization paper. He introduces an effective model that is valid only in a restricted domain, and then extends it over the whole Hilbert space without adjusting any of the interaction parameters. It is difficult to blame him, since the ideas of effective theory did not exist when he was working. Still, had he not been so busy with QED, perhaps he would instead have invented renormalisation as a way of rigorously introducing approximations in his quantum wire model, preempting the work of Wilson and saving physicists decades of uncertainty and controversy over the "hocus-pocus" (as Feynman put it) that was pre-Wilsonian renormalisation.

6.2 Microscopic system and relevant physics

We do not aim at generality in this chapter; rather, our intention is to investigate the relationship between microscopic physics and an effective model in a particular case, where such an investigation is analytically feasible. Hence, we work with a system that should be describable given knowledge of its microscopic two-body scattering properties. The system is composed of identical, weakly-interacting, spin-polarised fermions, obeying the Hamiltonian (5.1), and it is dilute in the sense that the use of a contact pseudopotential à la BEC theory is valid. Weak interactions are necessary so that the model's low-energy subspace is easily determined. Spin-polarisation is convenient, and helps to highlight the incongruity of interpreting g_4 as a measure of intrabranch scattering. Diluteness allows us to renormalise the model's parameters

in favour of two-body scattering data.

Given this setup, we now explore the two pieces of microscopic physics from which the system's effective low-energy behaviour will emerge. We begin by illustrating the importance of density waves.

6.2.1 Density waves

It is not immediately clear what should constitute a "density wave" in a quantum many-body system. We will take it to mean an oscillation of the density of the many-body wavefunction as one moves about in the many-body configuration space. Using this definition, the operator

$$\rho_k = \int dx\, e^{ikx} \psi^\dagger(x)\psi(x) \tag{6.2}$$

creates a density wave, where the wavelength of oscillations is $1/k$. To see this, it is easiest to consider the first-quantized situation, where ρ_k acts on an N-body state $\psi(x_1, ..., x_N)$ as

$$\rho_k \psi(x_1, ..., x_N) \propto \sum_{j=1}^{N} e^{ikx_j} \psi(x_1, ..., x_N). \tag{6.3}$$

The density of the new state is

$$|\rho_k \psi(x_1, ..., x_N)|^2 \propto \left[N + 2 \sum_{l<m} \cos(k(x_l - x_m)) \right] |\psi(x_1, ..., x_N)|^2. \tag{6.4}$$

We see that ρ_k modifies the density of ψ by a cosine in each of the relative coordinates, that is, it creates a density wave on top of the original state. It is easy to see that ρ_k has the following second-quantised representation in momentum space:

$$\rho_k = \sum_q c^\dagger_{k+q} c_q. \tag{6.5}$$

Let us now consider the weakly-interacting ground state, which, as we saw in the previous chapter, will contain particle-hole excitations above the Fermi sea, where none of the excitations are too energetic. Since all the action takes place near the Fermi points, it is a reasonable approximation to replace the quadratic dispersion

with a linear one, with slope v_F, when searching for the ground state. Writing $k = k_F + \tilde{k}$, one has

$$E(k) \approx \frac{\hbar^2 k_F^2}{2m} + v_F \tilde{k}. \tag{6.6}$$

where $v_F = \hbar k_F / m$ is the Fermi velocity. In this approximation, density waves are kinetic eigenstates:

$$\hat{H}_{\text{kin}} \rho_k |F\rangle = \left(\frac{\hbar^2 k_F^2}{2m} + v_F k \right) \rho_k |F\rangle. \tag{6.7}$$

This means that, instead of the c_k, we can use the ρ_k as "unperturbed" degrees of freedom, to be coupled together by the interaction. If this replacement significantly simplifies our model (and indeed it does) we will be justified in saying that the ρ_k represent physically relevant degrees of freedom.

If we are to reformulate our model in terms of density waves, clearly we should examine their commutation relations (we choose commutation rather than anti-commutation, because the relations will turn out to be approximately bosonic). Here we give quite a detailed treatment, since the result will be important for understanding the connection between Tomonaga's model and Luttinger's. The first step is to split ρ_k into left and right moving density waves:

$$\rho_k = \sum_{q>0} c^\dagger_{q+k} c_q + \sum_{q<0} c^\dagger_{q+k} c_q = \rho^+_k + \rho^-_k . \tag{6.8}$$

Here we lose the $q = 0$ state, but this is irrelevant for our treatment (it is a constant for charge-conserving systems). It is clear that ρ^+_k, ρ^-_k are also kinetic eigenstates, so our argument above applies to them just as well as it does to ρ_k. We calculate

$$[\rho^+_{k'}, \rho^+_k] = \sum_{q>0} \Xi(q - k') c^\dagger_{q+k} c_{q-k'} - \sum_{q>0} \Xi(q + k) c^\dagger_{k+k'+q} c_q, \tag{6.9}$$

were $\Xi(k)$ is the step function (we reserve θ for the scattering phase shift, which will be very important later). To simplify things, suppose that both k and k' are positive - the other cases lead to slightly different forms for the commutator, but

the following argument applies to all of them. Then we have

$$[\rho^+_{k'}, \rho^+_k] = \sum_{q=0}^{k'} c^\dagger_{q+k} c_{q-k'}. \tag{6.10}$$

Notice that this operator only affects states with momentum $\in (-k', k'+k)$, which will be important later. For k, k' sufficiently small, this operator vanishes when acting on the kinds of states we are interested in. To be precise, consider a state in which there are no holes deeper than $\alpha\, k_F$, where $0 < \alpha < 1$ (it makes sense to measure the position of the deepest hole this way, since whether we should consider a hole at some momentum k_0 to be "deep" or not depends on how large the Fermi momentum is). Then, if $k, k' < \alpha k_F/2$ and $k \neq -k'$, the commutator vanishes, since the creation operator always hits an occupied level. When $k = -k'$, the summand is the number operator, and since all the levels it hits are occupied, the sum is equal to k. Therefore, for small enough k, k', we have

$$[\rho^+_{k'}, \rho^+_k] = k\delta_{-k',k}. \tag{6.11}$$

Similarly, and under the same constraints on k, k', one can show that

$$[\rho^-_{k'}, \rho^-_k] = -k\delta_{-k',k}, \tag{6.12}$$

$$[\rho^-_{k'}, \rho^+_k] = 0. \tag{6.13}$$

We see that the left and right moving density waves obey bosonic commutation relations, if their momenta are small enough. As shown in Tomonaga's paper, writing the Hamiltonian in terms of these operators, with their commutators replaced by the bosonic ones given above, simplifies it greatly, to the extent that it is quite easily solvable (provided one also linearises the dispersion). We will not show this here. The argument is not very different from the bosonization of Luttinger's model described in the previous chapter. The reason we calculated the commutators explicity was to highlight the fact that there is a momentum scale, proportional to k_F, above which the bosonic description breaks down. Replacing the real commu-

tation relations for the density waves with their bosonic approximations over the whole Hilbert space is equivalent to taking this scale to infinity, that is, taking k_F to infinity. In fact, as we will see later, there exists a transformation on the model which takes k_F to infinity and simultaneously yields a linear dispersion relation. This transformation maps Tomonaga's model to Luttinger's.

To return to the original point, we stress that the model becomes very simple when written in terms of density waves and thus the $\rho_k^{(+,-)}$ represent important degrees of freedom, and we can expect them to play a prominent role in the low energy physics.

6.2.2 Interbranch scattering

Having argued that low-lying density wave excitations play a key role at low energies, let us try to understand which interaction processes are likely to be important. In the previous chapter, we enumerated the low-energy processes caused by a pairwise density-density interaction, and divided them into intrabranch and interbranch processes. One might imagine that all of the processes listed in that section play an important role in the low energy behaviour. It turns out, however, that only interbranch scattering is important in our system. This is because the phase shift for one-dimensional spin-polarized fermions vanishes in the zero relative momentum limit, as can be seen using the fact that $\sin(px) = px + \mathcal{O}(p^3)$ (using relative coordinates for a pair of particles) and the equivalent expansion for $\cos(px)$, and iterating Eq. (2.54), which gives

$$\psi_p(x)_{r\to\infty} = \frac{i\sin(px)}{\sqrt{2\pi}} - \frac{ipm}{\sqrt{2\pi}}\mathrm{sgn}(x)\int dx' x'^2 V_p(x') + \mathcal{O}(p^2). \tag{6.14}$$

Therefore, in the limit as $p \to 0$, we have

$$\theta_p = \arctan\left(\frac{pm}{\sqrt{2\pi}}\int dx' x'^2 V_p(x')\right), \tag{6.15}$$

$$= \frac{pm}{\sqrt{2\pi}}\int dx' x'^2 V_p(x') + \mathcal{O}(p^3), \tag{6.16}$$

$$\to 0. \tag{6.17}$$

Since low-energy intrabranch scattering occurs only between particles that are both near the same Fermi point, the relative momentum for such processes will be small, and the phase shift correspondingly negligible. Therefore, interbranch scattering is the only scattering process that can be expected to contribute significantly to the low-energy physics.

The situation can be summed up like this: at low energies, density wave excitations are kinetic eigenstates. They are the dispersing "particles" that get coupled by the interaction. This interaction, at low energies, consists only of interbranch scattering. Therefore, we identify the two pieces of physics that our effective model must reproduce as 1) the low-energy dispersion relation for density waves and 2) the interbranch scattering properties between the Fermi points. Having identified what we suppose to be the important low-energy physics, we may proceed with building our effective theory.

6.3 The effective interaction

We now begin constructing the effective model, requiring that it reproduces the microscopic density wave excitation energies and interbranch scattering properties between $\pm k_F$. As a first step, we introduce an effective interaction, which, since our system is dilute, we can take to be a contact-like interaction depending on a single parameter, g_2. Since we are working with spin-polarised fermions, however, there is a small subtlety. Due to the exclusion principle, the straightforward contact interaction has no effect, as may easily be seen in the principal value formalism. If $V(x) = \delta(x)$, one has $V_p(x) = \delta(x) - \delta(-x) = 0$. This does not mean we should abandon the idea of using a contact-like interaction, however; we just have to account for the antisymmetry of the fermionic wavefunction when defining the potential. This is best done via the second-quantised formalism, which is well-suited to dealing with symmetry issues. Writing the momentum-space first-quantised potential in second-quantised language, we have

$$\langle k'|V|k\rangle \equiv \langle 0|c_{l+2k'}c_l\hat{V}c_m^\dagger c_{m+2k}^\dagger|0\rangle, \tag{6.18}$$

where $\hat{V}$ is of the form (5.2), and l, m satisfy $m + k = l + k'$, ensuring conservation of momentum. From this one sees that the first-quantised potential must satisfy

$$\langle k'|V|k\rangle = -\langle -k'|V|k\rangle. \tag{6.19}$$

Thus, we can choose an effective potential that is essentially a contact interaction, but which is also a valid interaction for identical fermions satisfying (6.19), as follows:

$$\langle k|V|k'\rangle = g_2 \mathrm{sgn}(k)\mathrm{sgn}(k'). \tag{6.20}$$

The task now is to calculate the scattering properties due to this potential, yielding a value for g_2 in terms of the realistic phase shift. This might seem like an unnecessary step. After all, we still have to linearise the dispersion, which will - one would think - necessitate further renormalisation of g_2. However, our linearisation procedure will leave the interbranch phase shift of the quadratic model unchanged, and it is easier to calculate the phase shift with a quadratic dispersion than with a linear one. Therefore, we use (6.20) in (2.47), and, upon taking the momentum space representation and inspecting the k, k' dependence of $\mathcal{T}$, we discover that $\mathcal{T}(k, k', E) = \mathrm{sgn}(k)\mathrm{sgn}(k')\tau(E)$. Eq. (2.47) thus reduces to

$$\tau(E_k) = g_2 + \frac{g_2\tau(E_k)}{\sqrt{2\pi}}\,\mathcal{P}\int dq\,\frac{1}{E_k - E_q}. \tag{6.21}$$

The principal value integral vanishes, and so we have

$$\mathcal{T}(k, k', E) = g_2 \mathrm{sgn}(k)\mathrm{sgn}(k'). \tag{6.22}$$

Plugging the $\mathcal{T}$-matrix (6.22) into Eq. (2.36) and taking the position representation, we obtain

$$\psi_k(x) = \frac{i\sin(kx)}{\sqrt{2\pi}} + \mathrm{sgn}(k)\frac{img_2}{\sqrt{2\pi}}\,\mathcal{P}\int_0^\infty dq\,\frac{\sin(qx)}{k^2 - q^2}. \tag{6.23}$$

After a relatively simple but involved calculation, given in appendix B, we find the scattering state

$$\psi_k(x) = i\left(\frac{1}{\sqrt{2\pi}} - \frac{mg_2}{\sqrt{2\pi}\hbar^2|k|}\mathrm{Ci}(|kx|)\right)\sin(kx) - \frac{img_2}{\sqrt{2\pi}\hbar^2|k|}\mathrm{Si}(kx)\cos(kx), \quad (6.24)$$

where Ci and Si are the cosine and sine integrals respectively. To find the phase shift, we take the asymptotic limit. Using

$$\lim_{x\to\pm\infty}\mathrm{Ci}(x) = 0, \quad (6.25)$$

$$\lim_{x\to\pm\infty}\mathrm{Si}(x) = \pm\frac{\pi}{2}, \quad (6.26)$$

we obtain

$$\psi_k(x)_{x\to\infty} = i\frac{\sin(kx)}{\sqrt{2\pi}} - \frac{i\sqrt{\pi}mg_2}{2\sqrt{2}\hbar^2 k}\mathrm{sgn}(x)\cos(kx). \quad (6.27)$$

Comparing with Eq. (2.54), we find the phase shift

$$\tan(\theta_k) = -\frac{mg_2\pi}{2\hbar^2 k}. \quad (6.28)$$

In order for the effective model to reproduce realistic intrabranch scattering, it must give the correct phase shift for particles of relative momenta k_F. Therefore, the effective potential must be

$$\langle k|V|k'\rangle = -\frac{2\hbar^2 k_F}{m\pi}\tan(\theta_{k_F})\mathrm{sgn}(k)\mathrm{sgn}(k'), \quad (6.29)$$

where θ_{k_F} is the relevant realistic phase shift, which in most cases is readily calculated numerically. In the next section we find that the potential (6.29) reproduces the necessary scattering even after the dispersion relation has been linearised.

6.4 Linearising the dispersion

As we have seen, density waves play a fundamental role in the physics of 1D Fermi systems. The effective potential introduced in the last section has a very simple form

when written in terms of density waves, so that casting the effective model in terms of these excitations allows one to treat it easily. The kinetic term, however, acts on density waves in a complicated way, prohibiting a simple treatment of the bosonized model. The complexity is due to the fact that the dispersion is quadratic, so that the particle-hole pairs comprising a density wave (see Eq. (6.5)) each receive a different energy. This would not be so if the dispersion were linear. In that case, as we have seen, density waves on the Fermi sea would be kinetic eigenstates and the bosonized model easily solved. Since the dispersion for low-lying particle-hole excitations is approximately linear around k_F, and since, for weakly coupled systems, the kinetic term dominates the energetics, meaning that only density waves with small k will appear at low energies, we are in fact justified in using a linear dispersion to model the low-energy physics. Care must be taken when replacing the quadratic dispersion with a linear one, however. One must insure that the relevant physics is preserved. The most obvious way of doing this is to introduce a cutoff Λ in momentum space, restricting the Hilbert space so that $k \in (k_F - \Lambda, k_F + \Lambda) \cup (-k_F - \Lambda, -k_F + \Lambda)$, where the dispersion is approximately linear. This approach, while perfectly valid, does not yield an exactly solvable model. Density waves have only approximately-bosonic commutation relations, whereas exactly bosonic relations are necessary for solvability. Another idea would be to introduce a fully linear dispersion with no cutoff. This *would* give an exactly solvable model and is allowed as long as we preserve the relevant interbranch scattering properties and the dispersion relation of the density waves. Thus, we would have to to calculate the interbranch phase shift for a model with linear dispersion and adjust g_2 accordingly. This procedure is slightly problematic, however. From Eq. (6.21) one sees that the inverse T-matrix for such a model is ultraviolet divergent, so to proceed along these lines we would have to reintroduce the momentum cutoff, which we would then remove by renormalisation. The renormalisation procedure required here is somewhat unconventional, since the divergence arises from the dispersion rather than the interactions. Hence we will use an alternative method.

In Section 6.2.1 we showed that it is possible to construct a bosonic description of

our system, and that this description breaks down at a momentum scale proportional to k_F. We saw that the commutator $[\rho_k^+, \rho_{k'}^+]$ tries to create particle hole pairs between the momenta $-k'$ and $k' + k$, so it vanishes when $k \neq k'$ if there are no holes in that momentum range. This condition is satisfied if k' and k are sufficiently small compared with k_F, suggesting to us the possibly of constructing a model where $k_F = \infty$. Such a model will have the desired commutation relations for all k' and k. In fact, as we will now show, it is possible to do this in such a way that the resulting dispersion relation is exactly linear, and the necessary microscopic scattering and energetic properties are maintained.

To begin with, let us introduce a new Fermi momentum $\bar{k} \equiv \alpha k_F$. We parameterise $\bar{k}_F$ this way in order to keep track of the original k_F. We introduce the dispersion

$$E(k) = \frac{\hbar^2 k^2}{2m\alpha}. \tag{6.30}$$

We are interested in the behaviour around $\pm\bar{k}_F$, and so we write the momentum as

$$k = \Xi(k)\left(k_F\alpha + k_R\right) + \Xi(-k)\left(-k_F\alpha + k_L\right), \tag{6.31}$$

where $k_L \in (-\infty, \bar{k}_F)$ and $k_R \in (-\bar{k}_F, \infty)$. Here we have distinguished between left and right moving particles, of momentum k_L and k_R respectively, in our notation, in order to connect with Luttinger's model. Plugging this into Eq. (6.30), and taking the limit $\alpha \to \infty$, we arrive at the dispersion

$$E(k) = \frac{\hbar^2 k_F^2 \alpha}{2m} + v_F(\Xi(k)k_R - \Xi(-k)k_L). \tag{6.32}$$

The first, infinite term here does not depend on k. It is merely a chemical potential, and can be neglected for closed systems. We see, then, that α represents the extent to which the dispersion is linear. Taking it to infinity yields an exactly linear dispersion. Also, since the term linear in $\bar{k}$ has coefficient v_F, the dispersion correctly reproduces the microscopic kinetic energy for small excitations around k_F, as required. Since $\alpha \to \infty \Rightarrow \bar{k}_F \to \infty$, the density wave commutation relations will be exactly

bosonic for all momenta - this was verified in the last chapter. Replacing our original dispersion with the new one, our model becomes

$$H_\alpha = \sum_k \frac{\hbar^2 k^2}{2m\alpha} c_k^\dagger c_k + \hat{V}_{\text{eff}}. \tag{6.33}$$

From the last section and Eq. (6.28) in particular, we see that the two-body phase shift in this model is

$$\tan(\theta_k^{(\alpha)}) = -\frac{m\alpha g_2 \pi}{2\hbar^2 k}. \tag{6.34}$$

Notice the convenience of using a constant interaction: the phase shift at $k = \bar{k}_F$ is the same as the original phase shift at $k = k_F$.

$$\theta_{\bar{k}_F}^{(\alpha)} = \theta_{k_F}. \tag{6.35}$$

Thus, we have arrived at a linear dispersion without having to renormalise the interaction.

A couple of comments are in order at this point. Firstly, note that k_F depends on the particle density $\rho = N/L$ as $k_F = 2\pi\rho$. Thus, our new model, in having $\bar{k}_F \to \infty$, also has $\rho \to \infty$. But, the model is supposed to reproduce the physics of a dilute electron liquid, which seems incongruous. We are of course rescued by the fact that we have used a contact-like interaction in the effective model, rendering the system dilute at any density whatsoever. Also, the relation (6.31) between the original momenta and the k_L, k_R appearing in Luttinger's model, together with the aforementioned relation between ρ and k_F, can easily be seen to imply Eq. (5.42) from the previous chapter.

6.4.1 Tomonaga vs Luttinger

The procedure outlined above sheds some light on the relationship between Tomonaga's model and Luttinger's. In Tomonaga's paper, when approximately bosonic commutators are replaced by exactly bosonic relations and the dispersion is completely linearised, the above transformation is implicitly carried out. The full po-

tential is retained without change, however, which is not valid: in the transformed model one is interested in scattering between the points $k = \pm\infty$, where the potential may behave very differently from $k = \pm k_F$. If one wishes to use a non-constant potential, one must renormalise the theory upon the introduction of bosonic relations and a linear dispersion. In Luttinger's model, by contrast, one begins with a constant potential and two unbounded branches, which is precisely the $\alpha \to \infty$ limit of the model described above. We see that Luttinger's model can be thought of as a limiting case of Tomonaga's, where the commutation relations are exactly bosonic, and with an effective interaction that does not require renormalisation after the limiting process is carried out.

6.5 Intrabranch scattering in the effective model

We mentioned before that intrabranch scattering is not an important microscopic process. In this section, we show this fact to be crucial to the validity of Luttinger's model for spin-polarised fermions. While linearising the dispersion relation preserves interbranch scattering properties, it irrecoverably mangles intrabranch scattering: Luttinger's model simply does not have the capacity to reproduce microscopic intrabranch scattering physics. There are several ways of seeing this. As a heuristic argument, consider the linearisation technique described in the previous section, whereby the Fermi points are taken to infinity. One reason why interbranch scattering is invariant under this transformation is that the relevant relative momentum (this being k_F) also goes to infinity, whereas the relevant intrabranch momenta become vanishingly small compared with $\bar{k}_F$. To see the consequences of this, note that under the transformation (6.30) the two-body kinetic Hamiltonian becomes

$$H_0 = \frac{\hbar^2 k_F^2}{m} + \frac{\hbar^2 k_F K}{2m} + \frac{\hbar^2 K^2}{4m\alpha} + \frac{\hbar^2 k^2}{2m\alpha}, \tag{6.36}$$

where K is the total, and k the relative, momentum. The Green's function for the relative problem is thus

$$\langle x'|G_0(E_p - i\eta)|x\rangle = \int dp' \, \frac{e^{ip'(x-x')}}{\frac{\hbar^2 p^2}{2m\alpha} - i\eta - \frac{\hbar^2 p'^2}{2m\alpha}}. \tag{6.37}$$

For interbranch scattering the relevant energy is $E_{2k_F} = 2\alpha^2\hbar^2 k_F^2/m$, and one obtains

$$\langle x'|\mathcal{G}_0(E_{2k_F})|x\rangle = \frac{m}{2k_F}\sin(|k_F\alpha(x-x')|), \tag{6.38}$$

which is bound (though not convergent) as $\alpha \to \infty$. By contrast, a relative energy which does not scale with α, as for intrabranch scattering, gives

$$\langle x'|\mathcal{G}_0(E_p)|x\rangle = \frac{m\alpha\hbar}{|p|}\sin(|p\alpha(x-x')|), \tag{6.39}$$

which goes to infinity with α, indicating some pathology with the scattering theory in this limit.

This situation can be understood as a consequence of a general result concerning scattering in a flat band, which we prove now. The result is as follows: the stationary scattering states of a particle (or of the relative coordinate problem for a two-particle system) in a flat band can be written as

$$|k+\rangle = P_{I_0}|k\rangle \tag{6.40}$$

where I_0 is the space of eigenstates of V with vanishing eigenvalues, and P_{I_0} is the projector onto I_0. In the continuum the proof is simple: it is easy to show that the off-shell ($E \neq 0$) Green's function is given by

$$\langle x'|\mathcal{G}_0(E)|x\rangle = \frac{\delta(x-x')}{E} \tag{6.41}$$

in the flat band case. Using this in Eq. (2.48), one finds the scattering state

$$\psi_k(x) = \lim_{E\to 0} \frac{\phi_k(x)}{1 - \frac{V(x)}{E}}. \tag{6.42}$$

Clearly the relative energy of a pair of particles in a flat band is zero, so the on-shell limit is $E \to 0$. In this limit the scattering state vanishes, except at points where $V(x) = 0$, where it is equal to the incoming state; this is precisely the position-space version of the relation (6.40).

A more general proof is possible, which applies to any flat-banded system. Consider the off-shell Lippmann-Schwinger equation for $\mathcal{T}$, for two particles scattering in a flat band:

$$\langle k'|\mathcal{T}(E)|k\rangle = V(k',k) + \frac{1}{2\pi}\int_{-\infty}^{\infty} dq\, \frac{V(k',q)}{E}\langle q|\mathcal{T}(E)|k\rangle. \tag{6.43}$$

The $E \to 0$ limit can be determined by first noting that $\mathcal{T}$ inherits the analytic properties of the principal value interacting Green's function $\mathcal{G} = \Lambda G$, as is apparent from Eq. (2.14). In particular, for a non-vanishing potential, $\mathcal{G}$ is finite at $E = 0$, and thus, so is $\mathcal{T}$. This, together with Eq. (6.43), means that $\mathcal{T}$ has to vanish at least as fast as linearly as $E \to 0$. If it vanishes faster than linearly, however, Eq. (6.43) becomes $V(k',k) = 0$, which is not true. Therefore $\mathcal{T}$ vanishes linearly with E: $\mathcal{T}(E) = Et(0)$ for $E \to 0$. The Lippmann-Schwinger equation becomes

$$V(k',k) = -\frac{1}{2\pi}\int_{-\infty}^{\infty} dq\, V(k',q)\langle q|t(0)|k'\rangle. \tag{6.44}$$

The integral over q is merely a resolution of identity, hence the following operator relations hold:

$$V = -Vt(0), \tag{6.45}$$

$$\Rightarrow t^\dagger(0)V = -V, \tag{6.46}$$

where the latter identity makes clear that the columns of V are eigenvectors of $t^\dagger(0)$, with eigenvalues all equal to -1. In a basis where V is diagonal (in our case $\{|x\rangle\}$, but we denote the eigenvectors by $\{|\alpha_q\rangle\}$ to highlight the generality of the argument, which could for instance find application in lattice systems), we have

$$\langle \alpha_{q'}|t^\dagger(0)|\alpha_q\rangle = -\delta(\alpha_q - \alpha_{q'})\omega(\alpha_q) \tag{6.47}$$

where α_q is the eigenvalue of $|\alpha_q\rangle$. Clearly, $\omega(\alpha_q) = 2\pi$ as long as $\alpha_q \neq 0$. However, $\omega(0)$ is not fixed by this argument. Denoting the set of eigenvectors whose eigenvalues vanish as I_0, and its compliment by I_V, and inserting a resolution of identity into the Lippmann-Schwinger equation, we obtain

$$|k+\rangle = |k\rangle + \int_{-\infty}^{\infty} \frac{dk'}{2\pi} \left[\omega(0) \int_{I_0} \frac{dq'}{2\pi} \langle k'|\alpha_{q'}\rangle \int_{-\infty}^{\infty} \frac{dq}{2\pi} \langle \alpha_q|k\rangle - \int_{I_V} \frac{dq}{2\pi} \langle k'|\alpha_q\rangle\langle\alpha_q|k\rangle \right]. \tag{6.48}$$

Since $\omega(0)$ is arbitrary, we are free to set it to zero, which immediately yields (6.40). This result implies that there are only two S-matrices possible in a flat band, depending on whether one uses a finite or infinite range potential. For a finite range potential, it is clear that $S = 1$, while an infinite range potential gives $S = 0$, which is not an S-matrix at all. Thus, in a flat band, finite range scattering does not alter the incoming states, while infinite-range scattering is ill-defined.

To return to Luttinger's model; taking the $\alpha \to \infty$ limit in Eq. (6.36) gives a kinetic term that is independent of relative momentum. Therefore intrabranch scattering in this limit is equivalent to flat band scattering. Thus, assuming a finite range potential, we see that linearising the dispersion leads to a situation where intrabranch scattering essentially does not occur. Thankfully, this corresponds to the actual microscopic situation. If intrabranch scattering were an important process at the microscopic level, however, Luttinger's model would inevitably fail to reproduce it, and would thus give a poor description of the relevant physics.

6.6 Interpretation of phenomenological parameters

The picture painted in the last section is seemingly at odds with the usual interpretation of g_4. This is not yet a certainty, however: in order to rescue the interpretation, one might be tempted to set $g_4 = 0$, in which case it would correctly reflect the lack of intrabranch scattering. In this section, we show that setting g_4 to zero leads to a model that gives an incorrect dispersion relation for density wave excitations, and

hence fails to reproduce an important aspect of the microscopic physics.

That g_4 should be interpreted as an energy shift for excitations rather than a measure of scattering should not come as too great a surprise, given that the bosonic form of the intrabranch term, Eq. (5.29), is no different from the bosonised kinetic term, except that it appears multiplied by $g_4/2\pi$ rather than v_F. No matter what the microscopic interpretation of g_4 is, then, its role in the effective model must be to modify the speed of the bosons in some way. We can use this fact to calculate g_4 in terms of the realistic potential, by demanding that the density waves' microscopic kinetic behaviour is preserved in the effective model.

A little thought shows that this procedure is indeed necessary. The energy of density waves in the microscopic model depends not only on the kinetic term, but also on the interaction: a density wave with momentum q over the Fermi sea will have energy

$$E_q = \langle F|\rho_q^\dagger \left(H_0 + V\right) \rho_q|F\rangle. \tag{6.49}$$

If the ρ_q are to appear as fundamental degrees of freedom in the effective model, it is clearly important that their energies scale with q in the same way as in the microscopic model. To see why, let the effective dispersion for density waves be $\tilde{E}_q = \tilde{v}q$, whereas, for small q, their microscopic dispersion is $E_q = vq$. If $\tilde{v} > v$, for instance, then it will be more difficult for the interaction to create excitations in the effective model than in the microscopic model. Essentially, the effective theory will correspond to a microscopic system whose interactions are weaker than those of the system we are trying to model. Thus, it is important to ensure that, for small q, the microscopic dispersion E_q is preserved in the effective model. Since this dispersion depends on the interaction, one expects that the act of replacing the realistic two-body potential with the contact-like interaction (6.20) will change it. This change must therefore be corrected for, and we calculate this correction now, within the Hartree-Fock approximation.

To begin with, note that the energy of a density wave of small momentum is the same as that of a particle-hole pair near a Fermi point. Thus, consider the energy

expectation value of a low-lying particle-hole pair in the microscopic model,

$$\langle \tilde{k}+Q|H|\tilde{k}+Q\rangle = E_{FS} + \frac{\hbar^2}{2m}\left(Q^2 + 2\tilde{k}Q\right) + \langle \tilde{k}+Q|V|\tilde{k}+Q\rangle, \tag{6.50}$$

where $|\tilde{k}+Q\rangle \equiv c^\dagger_{\tilde{k}+q}c_k|F\rangle$ with $\tilde{k}$ slightly less than k_F, and Q such that $\tilde{k}+Q$ is slightly greater than k_F. Also, E_{FS} is the energy of the non-interacting Fermi sea. We have

$$\langle V\rangle = \frac{1}{2L}\sum_{kk'q} V(q)\langle c^\dagger_{k+q}c^\dagger_{k'-q}c_{k'}c_k\rangle \tag{6.51}$$

$$= \frac{1}{2L}\sum_{kk'q} \delta_{k',k+q}\langle c^\dagger_{k+q}c^\dagger_{k'-q}c_{k'}c_k\rangle \tag{6.52}$$

$$= -\frac{1}{2L}\sum_{k,q} V(k-q)\langle c^\dagger_q c_q c^\dagger_k c_k\rangle \tag{6.53}$$

$$= \frac{1}{L}\left(\sum_k V(\tilde{k}-k) - \sum_k V(\tilde{k}-k+Q) - \sum_{\substack{k=-k_F\\q=-k_F}}^{k_F}\frac{V(k-q)}{2}\right) \tag{6.54}$$

The last term in Eq. (6.54) does not depend on either $\tilde{k}$ or Q, and as such represents a constant contribution to the energy which, since we are only interested in the dispersion relation for particle-hole pairs, we may safely ignore. Thus, taking the limit $L\to\infty$, performing the resulting integral, and considering the limit of a low-lying particle hole pair, so that $\tilde{k}\approx k_F$ and $Q\approx 0$, we obtain

$$\langle V\rangle = \frac{Q}{2\pi}[V(0) - V(2k_F)]. \tag{6.55}$$

We now consider the same expectation value in the effective model, which is given by

$$\langle \tilde{k}+Q|H_{\text{eff}}|\tilde{k}+Q\rangle = v_F Q + \langle V_{\text{eff}}\rangle. \tag{6.56}$$

The second term is trivially evaluated by noticing that $V_{\text{eff}}(0) = V_{\text{eff}}(2k_F) = g_2$, so that by Eq. (6.55), which we derived without assuming anything about the

dispersion or the potential, $\langle V_{\text{eff}} \rangle = 0$. Ignoring constants, then, we have

$$\langle H - H_{\text{eff}} \rangle = \frac{Q}{2\pi}[V(0) - V(2k_F)]. \tag{6.57}$$

We see that the effective model does not produce the correct energetics for microscopic density waves. Not only is the energy incorrect, it is wrong by an amount that depends on the relative momentum between the particle-hole pairs comprising the waves. Clearly this situation is unacceptable; we can think of the effective model as it stands as having the wrong Fermi velocity. There is however a very simple remedy: one can introduce an effective, or renormalised, Fermi velocity to compensate. We define

$$v = v_F + \frac{g_4}{2\pi}, \tag{6.58}$$

with $g_4 = V(0) - V(2k_F)$. Replacing v_F with v in (5.32) yields a model that gives the correct excitation energy for the bosons.

It is obvious that g_4 does not vanish identically for any realistic interaction, given the way it depends on v_F. Therefore g_4 can in no way be thought of as a measure of intrabranch scattering in our model; it must instead be regarded purely as an energy shift exerted upon density waves by the full interaction. In fact, it can be seen from Eq. (6.18) that $\langle k_F|\hat{V}|k_F\rangle = V(0) - V(2k_F)$, i.e., g_4 is precisely the interaction matrix element governing *inter*branch scattering. In the first Born approximation $\mathcal{T} = V_p$, therefore, we have $g_4 = g_2$ (see Eq. (6.22)). Thus, we see that the energy shift is due primarily to interbranch interactions. In light of this, one sees that the usual fermionic form of Luttinger's Hamiltonian, which includes inter- and intrabranch scattering terms, is misleading in what it implies about the relationship between Luttinger's model and the underlying physics. We therefore propose an alternative Hamiltonian for the unbosonised fermionic effective theory, which emphasises the true physical role of g_4:

$$H_{\text{eff}} = v \sum_{k=-\infty}^{\infty} k \left[c^\dagger_{R,k} c_{R,k} - c^\dagger_{L,k} c_{L,k} \right] + V_{\text{inter}} \tag{6.59}$$

with

$$V_{\text{inter}} = \frac{g_2}{2L} \sum_{k,k',q} c^\dagger_{R,k} c_{R,k+q} c^\dagger_{k',L} c_{k'-q,L} + (R \leftrightarrow L), \tag{6.60}$$

and $v = v_F + g_4/2\pi$.

6.7 Summary and outlook

In this chapter we have essentially conducted a thought experiment, in order to test a widely-held interpretation of the phenomenological constants appearing in Luttinger's model. We considered a system of identical, spin-polarised fermions, and imagined it to be dilute enough so as to be describable via a simple pseudopotential, fit to two-body scattering data. We found fitting g_4 to intrabrach scattering data to be impossible, and concluded that the usual interpretation of g_4 as a measure of intrabranch scattering is untenable for the model under consideration, casting doubt upon the validity of the interpretation in general. Instead we showed that g_4 appears as a correcting factor, that must be added in by hand, to account for the energy shift exerted upon density waves by the realistic interaction, which disappears when one introduces the contact-like interaction necessary for successful bosonisation. On the other hand, our treatment shows that the usual interpretation of g_2 as a measure of interbranch scattering is perfectly sensible. We proved that g_2 may be fit to microscopic scattering data calculated using a fully quadratic dispersion and then used directly in the linearly-dispersing Luttinger model, since, as we showed, there exists a mapping between the quadratic and linear models which preserves interbranch scattering properties. A consideration of this mapping also highlighted a problem with Tomonaga's original treatment, and elucidated the relationship between his model and Luttinger's. We also proved a general result about scattering in a flat band; namely, that two-body scattering basically does not occur.

It would be interesting to discover how much of this picture holds true in more complex scenarios. One could for instance consider the intrabranch scattering of spinful fermions; to what extent does allowing for more than one scattering channel, and for mixed-symmetry wavefunctions, increase the intrabranch scattering ampli-

tude? Also, we have shown flat band scattering to be a rather strange process. Generalising to extra channels and exploring the three-body problem there may yield interesting results.

Appendix A

Ritz method

In this appendix we explain the variational Ritz method [94], which yields an approximation not only to the ground state, but also to the low-lying excitations and their energies. Consider the map from a Hilbert space $\mathcal{H}$ to the real numbers:

$$\mathcal{E}(|\psi\rangle) = \frac{\langle\psi|H|\psi\rangle}{\langle\psi|\psi\rangle}, \tag{A.1}$$

where H is a Hamiltonian operator. We claim that the extrema of this map lie along the eigenvectors of H, which we denote $|\,i\,\rangle$, so that $H_i|\,i\,\rangle = E_i|\,i\,\rangle$. To see this, it helps to use the $|\,i\,\rangle$ as a basis, writing $|\psi\rangle = \sum_i c_i|\,i\,\rangle$. One can think of the c_i as coordinates on $\mathcal{H}$, and in this coordinate system we have

$$\mathcal{E}(\mathbf{c}) = \frac{\sum_i |c_i|^2 E_i}{\sum_i |c_i|^2}. \tag{A.2}$$

We require the energies to be sorted: $E_0 < E_1 < E_2$ etc. Then, the function (A.2) takes its minimum value along the c_0 coordinate curve. The other extrema are saddle points: the function is maximum with respect to $\{c_i | i < j\}$ and minimum with respect to $\{c_i | i \geq j\}$ along the c_j coordinate curve. Since the c_i coordinate curves follow the directions of the eigenvectors $|\,i\,\rangle$, this proves our claim.

It is easy to verify the argument with a calculation. First of all, note that extremising $\mathcal{E}$ with respect to the coordinates c_i and doing so with respect to their

conjugates c_i^*, which is simpler, will yield the same answer. Also, we have

$$\langle\psi|\psi\rangle\partial_x\mathcal{E} = \partial_x\langle\psi|H|\psi\rangle - \mathcal{E}\partial_x\langle\psi|\psi\rangle, \tag{A.3}$$

where x is any coordinate, so the extrema of $\mathcal{E}$ satisfy

$$\partial_x\langle\psi|H|\psi\rangle - \mathcal{E}\partial_x\langle\psi|\psi\rangle = 0. \tag{A.4}$$

Then, we calculate

$$\partial_{c_i^*}\mathcal{E}(\mathbf{c}) = 0, \tag{A.5}$$

$$\Rightarrow c_i E_i - \frac{\sum_j c_j^* c_j E_j}{\sum_j c_j^* c_j} c_i = 0, \tag{A.6}$$

$$\Rightarrow E_i \sum_j c_j^* c_j - \sum_j c_j^* c_j E_j = 0. \tag{A.7}$$

This must hold $\forall i$ at an extremum. We therefore have a system of $\mathrm{Dim}(\mathcal{H})$ equations in $\mathrm{Dim}(\mathcal{H})$ variables, with a single solution. It is easy to see that $c_j^* c_j \propto \delta_{i,j}$ is a solution. Therefore it is the only solution, and we see that all the extrema of $\mathcal{E}$ do indeed lie along the directions of the energy eigenstates.

With the Ritz method one uses similar reasoning, but in a finite subspace of $\mathcal{H}$ (call it $\mathfrak{h}$), so that the extrema of $\mathcal{E}$ in $\mathfrak{h}$ can be calculated numerically. The idea is to choose $\mathfrak{h}$ so that it is close to the space of low-lying states. If this is done successfully, the extrema of $\mathcal{E}$ over $\mathfrak{h}$ will lie close to the true low-energy eigenstates. To see how this works, note that a choice of $\mathfrak{h}$ is essentially a guess at the subspace spanned by the lowest-lying $\mathrm{Dim}(\mathfrak{h})$ eigenstates. Ideally, one would guess correctly, $\mathfrak{h} = \mathrm{Span}(\ \{\,|\,i\,\rangle\ :\ i < \mathrm{Dim}(\mathfrak{h})\,\}\ )$, but of course in practice one is always somewhat off the mark. Let us capture the "wrongness" of the guess in vectors $|\alpha_i\rangle$, so that

$$\mathfrak{h} = \mathrm{Span}(\ \{\,|\,i\,\rangle + |\alpha_i\rangle\ :\ i < \mathrm{Dim}(\mathfrak{h})\,\}\ ). \tag{A.8}$$

It is convenient to choose the $|\alpha_i\rangle$ to be orthogonal to the true low-energy subspace,

which one can always do without loss of generality[1]. Then, we may write

$$|\alpha_i\rangle = \sum_{j \geq \mathrm{Dim}(\mathfrak{h})} \alpha_j^{(i)} |\, j \,\rangle. \tag{A.9}$$

We now take coordinates b_i on $\mathfrak{h}$, so that any state $|\psi\rangle \in \mathfrak{h}$ is written as

$$|\Psi\rangle = \sum_{i < \mathrm{Dim}(\mathfrak{h})} b_i \left(|\, i \,\rangle + \sum_{j \geq \mathrm{Dim}(\mathfrak{h})} \alpha_j^{(i)} |\, j \,\rangle \right). \tag{A.10}$$

Plugging this into Eq. (A.4), we obtain

$$\begin{aligned} &\left(b_i E_i + \sum_{\substack{i' < \mathrm{Dim}(\mathfrak{h}) \\ j \geq \mathrm{Dim}(\mathfrak{h})}} b_{i'} \alpha_j^{(i)} \alpha_j^{(i')} E_j \right) \sum_{i' < \mathrm{Dim}(\mathfrak{h})} b_{i'}^* b_{i'} \\ &\quad - \left(\sum_{i' < \mathrm{Dim}(\mathfrak{h})} b_{i'}^* b_{i'} E_{i'} + \sum_{\substack{i' < \mathrm{Dim}(\mathfrak{h}) \\ i'' < \mathrm{Dim}(\mathfrak{h}) \\ j \geq \mathrm{Dim}(\mathfrak{h})}} b_{i'}^* b_{i''} \alpha_j^{(i')} \alpha_j^{(i'')} E_j \right) b_i = 0 \end{aligned} \tag{A.11}$$

Arguing as before, this is a system of $\mathrm{Dim}(\mathfrak{h})$ equations in as many variables, of which $b_j \propto \delta_{i,j}$ is a - and therefore the only - solution. Thus, the extrema of $\mathcal{E}$ on the subspace $\mathfrak{h}$ lie along the directions $|\, i \,\rangle + |\alpha_i\rangle$. If one has made a good guess at the subspace, the $|\alpha_i\rangle$ will be small (in the sense of their norms), and so the extrema of $\mathcal{E}$ on $\mathfrak{h}$ will lie close to the true eigenstates: in other words, extremisng $\mathcal{E}$ with respect to a well-chosen ansatz will yield good approximations to the low-lying states.

We now show how to use this method to obtain the desired approximate states in practice. Let us choose a (not necessarily orthogonal) basis $\{|\psi_i\rangle\}$ for the guessed subspace $\mathfrak{h}$, and write $|\Psi\rangle = \sum_i b_i |\psi_i\rangle$. Plugging this into Eq. (A.4) yields

$$\sum_j \langle \psi_i | H | \psi_j \rangle b_j = E \langle \psi_i | \psi_j \rangle b_j. \tag{A.12}$$

This is nothing more than a generalised eigenvalue problem, for which numerous nu-

[1] To see this, let the $|\alpha_i\rangle$ point in any direction. Then, for instance, we can remove the $|1\rangle$ direction from $|0\rangle + |\alpha_0\rangle$ by subtracting $\langle 1|\alpha_0\rangle(|1\rangle + |\alpha_1\rangle)$. By repeatedly carrying out this kind of subtraction, one ends up with the desired basis.

merical routines for computing the $\mathrm{Dim}(\mathfrak{h})$ solution vectors and associated energies exist.

Appendix B

Asymptotic form of scattering wavefunction

Here we find the asymptotic form of the scattering state

$$\psi_k(x) = \frac{i\sin(kx)}{\sqrt{2\pi}} + \mathrm{sgn}(k)\frac{img_2}{\sqrt{2\pi}}\,\mathcal{P}\int_0^\infty dq\,\frac{\sin(qx)}{k^2-q^2}. \tag{B.1}$$

Essentially, this boils down to massaging the principal value integral into a state where the asymptotic limit can be easily taken. We label the integral $I_\mathcal{P}$ and write it as

$$I_\mathcal{P} = \frac{1}{2k}\mathcal{P}\int_0^\infty dq\left(\frac{\sin(qx)}{k-q} + \frac{\sin(qx)}{k+q}\right). \tag{B.2}$$

We focus on the first term for now. Adding zero in the form $kx-kx$ to the argument of the sine function and using a trigonometric identity, we have

$$\mathcal{P}\int_0^\infty dq\,\frac{\sin(qx)}{k-q} = \mathcal{P}\int_0^\infty dq\,\frac{\sin(x(k-q))\cos(kx)+\cos(x(k-q))\sin(kx)}{k-q}. \tag{B.3}$$

Focusing on the cosine term and abusing notation slightly,

$$\begin{aligned}\mathcal{P}\int_0^\infty dq\,\frac{\cos(x(k-q))}{k-q} = \\ \lim_{\epsilon\to 0^+}\left[\Xi(k)\left(\int_0^{k-\epsilon}+\int_{k+\epsilon}^\infty\right)+\Xi(-k)\int_0^\infty\right]dq\,\frac{\cos(x(k-q))}{k-q}.\end{aligned} \tag{B.4}$$

We deal with the last term first:

$$\int_0^\infty dq\,\frac{\cos(x(k-q))}{k-q} = -\int_{-\infty}^{k} dq\,\frac{\cos(qx)}{q} = \int_{-k|x|}^{\infty} dq\,\frac{\cos(q)}{q} = -\mathrm{Ci}(-k|x|). \quad \text{(B.5)}$$

Similarly, we have

$$\int_{k+\epsilon}^\infty dq\,\frac{\cos(x(k-q))}{k-q} = -\mathrm{Ci}(\epsilon|x|), \quad \text{(B.6)}$$

$$\int_0^{k-\epsilon} dq\,\frac{\cos(x(k-q))}{k-q} = \left(\int_{-\infty}^{k-\epsilon} - \int_{-\infty}^{0}\right) dq\,\frac{\cos(x(k-q))}{k-q} = \mathrm{Ci}(\epsilon|x|) - \mathrm{Ci}(k|x|). \quad \text{(B.7)}$$

Using these results in Eq. (B.4) yields

$$\mathcal{P}\int_0^\infty dq\,\frac{\cos(x(k-q))}{k-q} = -\Xi(k)\mathrm{Ci}(k|x|) - \Xi(-k)\mathrm{Ci}(-k|x|) = -\mathrm{Ci}(|kx|). \quad \text{(B.8)}$$

By similar calculations, one can show that:

$$\mathcal{P}\int_0^\infty dq\,\frac{\cos(x(k+q))}{k+q} = -\mathrm{Ci}(|kx|) \quad \text{(B.9)}$$

$$\mathcal{P}\int_0^\infty dq\,\frac{\sin(x(k+q))}{k+q} = \mathcal{P}\int_0^\infty dq\,\frac{\sin(x(k-q))}{k-q} = -\mathrm{Si}(kx) \quad \text{(B.10)}$$

Thus, from Eq. (B.2), we see that

$$I_{\mathcal{P}} = -\frac{1}{k}\left[\mathrm{Ci}(|kx|)\sin(kx) + \mathrm{Si}(kx)\cos(kx)\right], \quad \text{(B.11)}$$

which we use in Eq. (6.23), obtaining

$$\psi_k(x) = i\left(\frac{1}{\sqrt{2\pi}} - \frac{mg_2}{\sqrt{2\pi}\hbar^2|k|}\mathrm{Ci}(|kx|)\right)\sin(kx) - \frac{img_2}{\sqrt{2\pi}\hbar^2|k|}\mathrm{Si}(kx)\cos(kx), \quad \text{(B.12)}$$

which is the desired result from which the asymptotic form is easily found.

Bibliography

[1] S. Tomonaga, Prog. Theor. Phys. **5**, 544 (1950)

[2] L. D. Landau, J. Exptl. Theoret. Phys. **30**, 1058 (1956)

[3] E. H. Lieb and D. C. Mattis, *Mathematical Physics in One Dimension*, Elsevier (1966)

[4] S. Schmid, G. Thalhammer, K. Winkler, F. Lang, and J. H. Denschlag, New J. Phys. **8**, 159 (2006)

[5] C.-C. Chien, M. Di Ventra, Phys. Rev. A **87**, 023609 (2013)

[6] M. Köhl, T. Stöferle, H. Moritz, C. Schori, and T. Esslinger, Appl. Phys. B **79**, 1009 (2004)

[7] D. Laroche, G. Gervais, M. P. Lilly, and J. L. Reno, Science **343**, 631 (2014)

[8] F. Hirler, J. Smoliner, E. Gornik, G. Weimann, and W. Schlapp, Appl. Phys. Lett. **57**, 261 (1990)

[9] M. Bockrath, D. H. Cobden, J. Lu, A. G. Rinzler, R. E. Smalley, L. Balents, and P. L. McEuen, Nature **397**, 598 (1999)

[10] A. Altland and B. Simons, *Condensed Matter Field Theory*, Cambridge University Press (2010)

[11] X. -G. Wen, *Quantum Field Theory of Many-Body Systems*, Oxford University Press (2004)

[12] A. M. Tsvelik, *Quantum Field Theory of Condensed Matter Physics*, Cambridge University Press (2007)

[13] E. Witten, *Three Lectures on Topological Phases of Matter*, arXiv: 1507.07798 (2015)

[14] J. E. Avron, D. Osadchy, and R. Seiler, Physics Today **56**, 38 (2005)

[15] P. Sinjukow and W. Nolting, Phys. Rev. B **65**, 212303 (2002)

[16] S. D. Huber and E. Altman, Phys. Rev. B **82**, 184502 (2010)

[17] J. Taylor, *Scattering Theory*, John Wiley, (2002)

[18] C. J. Joachian, *Quantum Collision Theory*, North-Holland Pub. Co. (1976)

[19] R. Pike and P. Sabatier (Eds.) *Scattering*, Elsevier (2002)

[20] B. Blanchard, *Mathematical Methods in Physics*, Birkhauser (2003)

[21] Y. Castin and J. Dalibard, EPL **14**, 761 (1991)

[22] R. P. Feynman, Found. Phys. **16**, 507 (1986)

[23] I. Bloch, Nat. Phys. **1**, 23 (2005)

[24] J. Simon, W. S. Baker, R. Ma, M. E. Tai, P. M. Preiss, and M. Greiner, Nature **472**, 307 (2011)

[25] I. Bloch, J. Dalibard, and S. Nascimbene, Nat. Phys. **8**, 267 (2012)

[26] J. Struck, C. Ölschläger, R. Le Targat, P. Soltan-Panahi, A. Eckardt, M. Lewenstein, P. Windpassinger, and K. Sengstock, Science **333**, 996 (2011)

[27] T. Kinoshita, T. Wenger, and T. Weiss, Nature **429**, 277 (2004)

[28] S. Yi, T. Li, and C. P. Sun, Phys. Rev. Lett. **98**, 260405 (2007)

[29] N. Goldman, J. C. Budich, and P., Zoller, Nat. Phys. **12**, 639 (2016)

[30] P.-I. Schneider and A. Saenz, Phys. Rev. A **85**, 050304R (2012)

[31] M. Takamoto, F.-L. Hong, R. Higashi, and H. Katori, Nature **435**, 321 (2005)

[32] M. Lewenstein, A. Sanpera, and V. Ahufinger, *Ultracold atoms in optical lattices*, Oxford University Press (2012)

[33] D. Jaksch, C, Bruder, J. I. Cirac, C. W. Gardiner, and P. Zoller, Phys. Rev. Lett. **81**, 3108 (1998)

[34] K. Noda, K. Inaba, and M. Yamashita, Phys. Rev. A **90**, 043624 (2014)

[35] M. Metcalf, G.-W. Chern, M. Di Ventra, and C.-C. Chien, J. Phys. B **49**, 075301 (2016)

[36] L. Zheng, L. Feng, and W. Yong-Shi, Chin. Phys. B **23**, 077308 (2014)

[37] T. Zhang and G. -B. Jo, Sci. Rep. **5**, 16044 (2015)

[38] K. Rzazewski and R. W. Boyd, J. Mod. Opt. **20** 1137 (2004)

[39] N. Marzari, A. A. Mostofi, J. R. Yates, I. Souza, and D. Vanderbilt, Rev. Mod. Phys. **84**, 1419 (2012)

[40] C. Chin, R. Grimm, P. Julienne, and E. Tiesinga, Rev. Mod. Phys. **82**, 1225 (2010)

[41] G. Grishkevich, S. Sala, and A. Saenz, Phys. Rev. A **84**, 062710 (2011)

[42] A. Eckardt, P. Hauke, P. Soltan-Panahi, C. Becker, K. Sengstock, and M. Lewenstein, EPL **89**, 10010 (2010)

[43] M. Bukov, L. D'Alessio, and A. Polkovnikov, Adv. Phys. **64**, 139 (2015)

[44] A. Eckardt and M. Holthaus, Phys. Rev. Lett. **95**, 260404 (2005)

[45] H. Linger, C. Sias, D. Ciampini, Y. Singh, A. Zenesini, O. Morsch, and E. Arimondo, Phys. Rev. Lett. **99**, 220403 (2007)

[46] N. Goldman and J. Dalibard, Phys. Rev. X **4**, 031027 (2014)

[47] R. Graham, M. Schlautmann, and P. Zoller, Phys, Rev. A **45**, R19 (1992)

[48] K. W. Madison, M. C. Fischer, R. B. Ciener, Q. Niu, and M. G. Raizen, Phys. Rev. Lett. **81**, 5093 (1998)

[49] M. Valiente and N. T. Zinner, preprint arXiv:1611.05459

[50] E. H. Lieb, Phys. Rev. Lett. **62**, 1201 (1989)

[51] A. Mielke, Phys. Lett. A **174**, 443 (1993)

[52] H. Tasaki, Prog. Theor. Phys. **99**, 489 (1998)

[53] S. Miyahara, S. Kusuta, and N. Furukawa, Physica C **460**, 1145 (2007)

[54] K. Sun, Z. Gu, H. Katsura, and S. Das Sarma, Phys. Rev. Lett. **106**, 236803 (2011)

[55] Y. F. Wang, A.-C. Gu, C.-D. Gong, and D. N. Sheng, Phys. Rev. Lett. **107**, 146803 (2011)

[56] D. N. Sheng, Z.-C. Gu, K. Sun, and L. Sheng, Nat. Comm. **2**, 389 (2011)

[57] S. Flach, D. Leykam, J. D. Bodyfelt, P. Matthies, and A. S. Desyatnikov, EPL **105**, 30001 (2014)

[58] S. R. White, Phys. Rev. Lett. **69**, 2863 (1992)

[59] G. De Chiara, M. Rizzi, D. Rossini, and S. Montanegro, J. Comput. Theor. Nanosci. **5**, 1277 (2008)

[60] The routine we used is documented on the GSL website: www.gnu.org/software/gsl/manual. The solver function is named gsl_eigen_genv.

[61] B. Paredes, A. Widera, V. Murg, O. Mandel, S. Fölling, I. Cirac, G. V. Shlyapnikov, T. W. Hänsch, and I. Bloch, Nature **429**, 277 (2004)

[62] I. Bloch, J. Dalibard, and W. Zwerger, Rev. Mod. Phys. **80**, 885 (2008)

[63] P. Longo and J. Evers, Phys. Rev. Lett **112**, 193601 (2014)

[64] J. M. Luttinger, J. Math. Phys. **4**, 1154 (1963)

[65] J. von Delft and H. Schoeller, Ann. Phys. **7**, 225 (1998)

[66] S. Eggert, *Lecture notes from the A3 Foresight Summer School, Korea* in: "Theoretical Survey of One Dimensional Wire Systems", Y. Kuk, et al. (Eds.), (Sowha Publishing, Seoul, 2007); arXiv:0708.0003.

[67] J. W. Negele and H. Orland, *Quantum Many-Particle Systems*, Addison-Wesley (1998)

[68] Y. Tserkovnyak, B. I. Halperin, O. M. Auslaender, and A. Yacoby, Phys. Rev. B **68**, 125312 (2003)

[69] O. Auslaender, A. Yacoby, R. De Picciotto, K. W. Baldwin, L. N. Pfeiffer, and K. W. West, Science **295**, 825 (2002)

[70] Z. Yao, H. W. Ch. Postma, L. Balents, and C. Dekker, Nature **402**, 273 (1999)

[71] D. C. Mattis and E. H. Lieb, J. Math. Phys. **6**, 304 (1965)

[72] A. Overhauser, *Physics* **1**, 307 (1965)

[73] F. D. M. Haldane, J. Phys. C: Solid State Phys. **14**, 2585 (1981); Phys. Rev. Lett. **45**, 1358 (1980)

[74] J. Sirker, Int. J. Mod. Phys. B **26**, 1244009 (2012)

[75] V. Mastropietro, *Luttinger Model: The First 50 Years and Some New Directions*, World Scientific (2014)

[76] A. D. Maestro and I. Affleck, Phys. Rev. B **82**, 060515(R) (2010)

[77] C. Karrasch, J, Rentrop, D. Schuricht, and V. Meden, Phys. Rev. Lett. **109** 126406 (2012)

[78] S. Tarucha, T. Honda, and T. Saku, Solid State Commun. **94**, 413 (1995)

[79] M. Bockrath, D. H. Cobden, J. Lu, A. G. Rinzler, R. E. Smalley, L. Balents, and P. L. McEuen, Nature **397**, 598 (1999)

[80] Z. Shi, X. Hong, H. A. Bechtel, B. Zeng, M. C. Martin, K. Watanabe, T. Taniguchi, Y.-R. Shen, and F. Wang, Nat. Photonics **9**, 515 (2015)

[81] H.Ishii, H. Kataura, H. Shiozawa, H. Yoshioka, H. Otsubo, Y. Takayama, T. Miyahara, S. Suzuki, Y. Achiba, M. Nakatake, T. Narimura, M. Higashiguchi, K. Shimada, H. Namatame, and M. Taniguchi, Nature **426**, 540 (2003)

[82] S. V. Zaitsev-Zotov, Y. A. Kumzerov, Y. A. Firsov, and P. Monceau, J. Phys **12**, L303 (2000)

[83] A. M. Chang, L. N. Pfeiffer, and K. W. West, Phys. Rev. Lett. **77**, 2538 (1996)

[84] F. Liu, M. Bao and K. L. Wang, Appl. Phys. Lett. **86**, 213101 (2005)

[85] E. Haller, R. Hart, M. J. Mark, J. G. Danzl, L. Reichsöllner, M. Gustavsson, M. Dalmonte, G. Pupillo, and H. C. Hägerl, Nature **466**, 597 (2010)

[86] H. Bruus and K. Flensberg, *Many-body Quantum Theory in Condensed Matter Physics*, Oxford University press (2004)

[87] J. Voit, Rep. Prog. Phys **58**, 9 (1995)

[88] A. E. Mattsson, S. Eggert, and H. Johannesson, Phys. Rev. B **56**, 15615 (1997)

[89] S. Ejuma and H. Fehske, EPL **87** 27001 (2009)

[90] O. M. Sule, H. J. Changlani, I. Maruyama, and S. Ryu, Phys. Rev. B **92**, 075128 (2015)

[91] K. Hattori and A. Rosch, Phys. Rev. B **90**, 115103 (2014)

[92] D. Morath, N. Sedlmayr, J. Sirker, and S. Eggert, Phys. Rev. B **94**, 115162 (2016)

[93] M. Valiente and P. Öhberg, Phys. Rev. A **94**, 051606(R) (2016)

[94] A. Messiah, *Quantum Mechanics, Volume 2*, North-Holland (1981)

List of Figures